REVIEW

The anaerobic soil volume as a controlling factor of denitrification: a review

Steffen Schlüter[1] · Maik Lucas[1,2] · Balazs Grosz[3] · Olaf Ippisch[4] · Jan Zawallich[5] · Hongxing He[6] · Rene Dechow[3] · David Kraus[7] · Sergey Blagodatsky[8] · Mehmet Senbayram[9] · Alexandra Kravchenko[10] · Hans-Jörg Vogel[1] · Reinhard Well[3]

Abstract

Denitrification is an important component of the nitrogen cycle in soil, returning reactive nitrogen to the atmosphere. Denitrification activity is often concentrated spatially in anoxic microsites and temporally in ephemeral events, which presents a challenge for modelling. The anaerobic fraction of soil volume can be a useful predictor of denitrification in soils. Here, we provide a review of this soil characteristic, its controlling factors, its estimation from basic soil properties and its implementation in current denitrification models. The concept of the anaerobic soil volume and its relationship to denitrification activity has undergone several paradigm shifts that came along with the advent of new oxygen and microstructure mapping techniques. The current understanding is that hotspots of denitrification activity are partially decoupled from air distances in the wet soil matrix and are mainly associated with particulate organic matter (POM) in the form of fresh plant residues or manure. POM fragments harbor large amounts of labile carbon that promote local oxygen consumption and, as a result, these microsites differ in their aeration status from the surrounding soil matrix. Current denitrification models relate the anaerobic soil volume fraction to bulk oxygen concentration in various ways but make little use of microstructure information, such as the distance between POM and air-filled pores. Based on meta-analyses, we derive new empirical relationships to estimate the conditions for the formation of anoxia at the microscale from basic soil properties and we outline how these empirical relationships could be used in the future to improve prediction accuracy of denitrification models at the soil profile scale.

Keywords Anoxic microsites · Anaerobic balloon · N_2O emissions · Product ratio · X-ray CT · Oxygen sensors

---

✉ Steffen Schlüter
steffen.schlueter@ufz.de

1. Helmholtz-Centre for Environmental Research – UFZ, Soil System Sciences, Halle, Germany

2. Institute of Ecology, Chair of Soil Science, Technical University of Berlin, Berlin, Germany

3. Thünen Institute of Climate-Smart Agriculture, Brunswick, Germany

4. Scientific Computing, Technical University of Clausthal, Clausthal, Germany

5. Department of Mathematics, Technical University of Munich, Garching, Germany

6. McGill University, Geography, Montreal, Canada

7. Karlsruhe Institute of Technology KIT, Atmospheric Environmental Research, Garmisch-Partenkirchen, Germany

8. Terrestrial Ecology Group, Institute of Zoology, University of Cologne, Cologne, Germany

9. Plant Nutrition and Soil Science, Harran University, Sanliurfa, Turkey

10. Department Plant, Soil and Microbial Sciences, Alexandra Kravchenko, Michigan State University, East Lansing, USA

🌀 Springer

Introduction

Denitrification in soil fuels global warming and the loss of reactive nitrogen (N) to the atmosphere. Global denitrification rates have been increased by approximately 20% since preindustrial times (Galloway et al. 2004; Schlesinger 2009) and the N_2O emissions as a by-product of denitrification have increased atmospheric concentrations by 2% per decade over the last four decades, mainly due to soil N_2O emissions from agriculture (Tian et al. 2020). Denitrification is a microbial respiratory process that uses nitrogen species as electron acceptors and involves a cascade of reduction steps from soluble nitrate (NO_3^-) via intermediates (NO_2^-, NO, N_2O) to gaseous dinitrogen (N_2) (Philippot et al. 2007; Zumft 1997). Soil denitrification requires the presence of suitable electron donors (e.g. organic carbon), nitrogen species (mainly nitrate), the shortage of oxygen as the predominant electron acceptor and a microbial community with the metabolic capacity to denitrify (Firestone 1982; Philippot et al. 2007; Robertson and Groffman 2007).

The timing and magnitude of N_2O emissions are notoriously difficult to predict, leading to considerable uncertainty in N budgets and ecosystem modelling (Groffman et al. 2009; Tian et al. 2020). The difficulty in prediction is due to the fact that denitrification in most soils, particularly in the well aerated uplands, occurs within sub-cm to few-cm sized microsites (Robertson 2023). The denitrification hotspots are rich in labile carbon and nitrogen species but poor in oxygen, despite the presence of oxygen everywhere else in the soil; they are transient in nature, and can be extremely variable in time and space. The variability is due to the interplay of the abovementioned denitrification prerequisites. For example,

i) Denitrification completeness, often expressed by the product stoichiometry, $N_2O/(N_2O + N_2)$, can vary widely in soils depending on environmental factors. Low temperature (Holtan-Hartwig et al. 2002), low pH (Bakken et al. 2012; Čuhel and Šimek 2011; Šimek and Cooper 2002; Xu et al. 2023), copper deficiency (Shen et al. 2020), and nitrate excess (Iqbal et al. 2015; Senbayram et al. 2019; Weier et al. 1993) can reduce denitrification completeness. Water excess near full saturation (Friedl et al. 2016; Guo et al. 2014) and prolonged anaerobic conditions (Friedl et al. 2016; Senbayram et al. 2022; Weier et al. 1993) can increase it. Of these contributors, only soil temperature can be expected to vary in a predictable manner across the soil profile, while the remaining soil properties can vary widely within just a few mm to a few cm of intact soil matrix.

ii) Denitrification completeness also depends on the abundance of organisms capable of completing the final denitrification step (Cavigelli and Robertson 2001;

Philippot et al. 2011). Furthermore, there are different regulatory phenotypes that alter the timing and magnitude of intermediates (Bergaust et al. 2011), and the heterogeneous distribution of microorganisms in space is notorious (Bach et al. 2018). Both the normalized abundance of denitrification genes (Schlatter et al. 2019) and the denitrification potential (Casey et al. 2004) have been reported to be greater in the vicinity of earthworm burrows and other macropores, suggesting that the soil microstructure may have a lasting effect on patterns of denitrification activity.

iii) Just because soil turns anoxic during wetting and switches to anaerobic respiration, does not mean that denitrification will occur, as nitrate can be limiting (Højberg et al. 1994; Myrold and Tiedje 1985).

iv) When all other conditions are met, denitrification, in contrast to iron or sulfate reduction, occurs regardless of the quality of organic carbon, i.e. the degree of reduction (Keiluweit et al. 2016; Lacroix et al. 2023). However, the high microbial activity in hotspots fueled by easily degradable organic compounds facilitates denitrification due to local oxygen shortage in otherwise well-aerated soils. These hotspots formed on decomposing plant or animal residues can be a major driver of uncertainty in N_2O emissions (Parkin 1987).

Although the presence of microbial hotspots and their heterogeneous distribution in soil are generally accepted (Groffman et al. 2009; Kuzyakov and Blagodatskaya 2015), there are knowledge gaps especially at small spatial scales, that currently hinder a better representation of such hotspots in the predictive modelling of denitrification. Locations of denitrification activity are typically conceptualized as the anaerobic soil volume (Arah and Smith 1989) or an anaerobic balloon that can expand or deflate with oxygen availability (Li et al. 1992), without reference to a specific location or soil structural properties. Conceptual ideas on how the anaerobic soil volume is modulated by soil structure heterogeneity are few and have not yet been implemented in common ecosystem models.

Here, we review the recent advances in the quantification of the anaerobic soil volume fraction using various experimental approaches and synthesize some pertinent relationships of the anaerobic soil volume with more readily available state variables through an extensive literature review. We conducted meta-analyses focusing on i) the critical air distances in soil leading to the formation of anoxia and ii) the anaerobic soil volume fraction estimated from oxic and anoxic incubations. Based on the results, we propose a new concept for including denitrification in process models operating at relevant scales such as that of a soil profile. This review is primarily concerned with

the effect of the anaerobic soil volume on denitrification. However, we refer to previous reviews and meta-studies covering other important aspects of denitrification such as controlling factors (Butterbach-Bahl et al. 2013; Li et al. 2022; Saggar et al. 2013), measurement techniques (Friedl et al. 2020; Groffman et al. 2006; Micucci et al. 2023) and modeling approaches (Blagodatsky and Smith 2012; Butterbach-Bahl et al. 2013; Grosz et al. 2021; Wang et al. 2021), as well as the role of anaerobic microsites for matter cycling beyond denitrification (Keiluweit et al. 2016; Lacroix et al. 2023).

Factors controlling anaerobic soil volume

Impact of water

Microbial activity in general, and denitrification in particular, is highly dependent on soil water content (Linn and Doran 1984; Moyano et al. 2013; Skopp et al. 1990). Water is an essential requirement for microbial life in soil, a constituent of cells, a solvent, and a transport medium of soluble substrates. As a consequence, soil microbial activity decreases linearly with the decreasing logarithm of water potential in a range between field capacity and permanent wilting point (Manzoni et al. 2012). Similarly, microbial activity may be reduced toward full water saturation as water can block air continuity in soil pores, thereby limiting oxygen supply. Air continuity is important for soil aeration as oxygen diffusion in water is about 10,000 times slower than in the air (Currie 1961). Relative gas diffusivity, defined as the ratio between gas diffusivity in soil and air, may therefore be a better, less site-dependent predictor of denitrification than water content (Andersen and Petersen 2009; Balaine et al. 2013; Mutegi et al. 2010; Petersen et al. 2008). The optimal soil moisture for microbial activity with unrestricted water and oxygen supply is soil-dependent with a rather broad plateau around 50 – 60% water-filled pore space (WFPS), or a matric potential range around field capacity, i.e. around pF 2 (Ghezzehei et al. 2019; Moyano et al. 2013), or a relative gas diffusivity greater than 0.015 – 0.02 (Li et al. 2021; Stepniewski 1980). The moisture level at which intensive denitrification sets in ranges broadly around 70% WFPS and varies among soils (Bateman and Baggs 2005; Cardenas et al. 2017; Castellano et al. 2010; Gillam et al. 2008; Linn and Doran 1984; Rohe et al. 2021; Ruser et al. 2006; Weier et al. 1993; Werner et al. 2014). Alternatively, denitrification begins at a relative gas diffusivity of 0.005 – 0.01, a range that is narrower and less soil-dependent than the range of soil moisture (Balaine et al. 2013; Chamindu Deepagoda et al. 2019; Li et al. 2021; Owens et al. 2017; Rousset et al. 2020) though higher values have also been reported (Petersen et al. 2013).

A reason for this broad moisture transition range rather than a sharp moisture threshold is that at low water saturation the anaerobic soil volume might emerge in a few anoxic microsites with high oxygen consumption in an otherwise well-aerated soil. As the water content increases, the diffusive oxygen supply goes down and the anaerobic soil volume may gradually spread into larger areas with lower oxygen consumption rates.

Impact of spatial heterogeneity

Oxygen availability in soils results from a delicate balance between oxygen consumption and replenishment. This has been shown by numerous soil incubation studies under different temperatures and water contents or external oxygen concentrations (Schaufler et al. 2010; Silvennoinen et al. 2008; Veraart et al. 2011; Werner et al. 2014; Zhu et al. 2013). The total oxygen supply and demand in soil is heterogeneously distributed. Even if the overall water content and substrate availability are the same, the denitrification rates and kinetics can be very different depending on the spatial distribution patterns of microbial hotspots (Schlüter et al. 2019; Zhu et al. 2015). Denitrification hotspots are typically formed around decomposing plant residues (Højberg et al. 1994; Kravchenko et al. 2017; Parkin 1987), and sometimes almost all N_2O production can originate from a very small fraction of the soil volume (Parkin 1987). The distribution patterns of air-filled pores and organic residues are not random, but are imposed by soil structure. That is, the air-filled pore space at a given matric potential can have different spatial configurations depending on how the pores were formed, e.g. by biotic processes like bioturbation, abiotic processes like wetting–drying cycles or technical processes like tillage. As a consequence, the diffusion distances of dissolved oxygen through the wet soil matrix can be very different depending on the soil management (see the case study on plowed cropland soil and no-till grassland soil below) (Lucas et al. 2023a; Schlüter et al. 2020). X-ray microtomography has been used repeatedly as a means of determining the volume fraction and distribution of air-filled pores to help predicting N_2O emissions (Lucas et al. 2023a; Porre et al. 2016; Rabot et al. 2015; Rohe et al. 2021).

Particulate organic matter (POM) is also not randomly distributed within the soil matrix, but can be thoroughly mixed into the wet soil matrix or mainly located in air-filled macropores, depending on soil structure formation. A large fraction of POM originates from roots and, since roots grow into larger pores or produce their own biopores (Lucas et al. 2019, 2023b), such POM fragments are typically located in close proximity to air-filled macropores (Kravchenko et al. 2018b; Schlüter et al. 2022). The size, shape, and pore distances of individual POM fragments change with POM aging and occlusion during soil structure turnover (Schlüter et al. 2022). At the scale of a soil horizon, under constant land use and organic matter supply, a reasonably stable, site-specific distribution of these POM properties should evolve,

resulting in characteristic denitrification activities under wet conditions. The size and physical characteristics of POM are also important determinants of how much N_2O is produced and influence the dominant pathways of its production within the soil matrix. The larger the POM fragment, the more decoupled from the surrounding soil matrix it may be in terms of the microenvironment it provides to the resident microorganisms. The effects of POM size may be particularly pronounced on water content, oxygen availability, and spatio-temporal patterns of oxygen distribution within and around POM. Larger POM fragments absorb more water from the surrounding soil (Iqbal et al. 2013). The resulting greater activity of microbial decomposers (Kravchenko et al. 2018a; Loecke and Robertson 2009) leads to oxygen depletion and a spread of anaerobic conditions. The bigger the volume of C- and N-rich substrate under anaerobic conditions, the greater is denitrification (Robertson 2023). Water absorption by POM and subsequent anaerobic conditions may also depend on the water holding capacity of POM (Kravchenko et al. 2018a) – the higher it is, the greater is the spatial and temporal extent of denitrification.

Impact of events and time

Both oxygen demand and oxygen supply can change very rapidly, leading to abrupt changes in the anaerobic soil volume and creating ephemeral events or "hot moments" of denitrification. The hot moments, i.e. extremely high emission events occurring in very short periods of time, can account for a dominant portion of the annual N_2O emissions (Butterbach-Bahl et al. 2013; Groffman et al. 2009; Song et al. 2019). Three typical situations are known to trigger large denitrification pulses (Groffman et al. 2009). First, spring thaw events can release a substantial fraction of the annual gaseous denitrification products (Wagner-Riddle et al. 2017). This is due to the release of large amounts of labile carbon substrates accumulated during winter, while simultaneously inducing high water contents for prolonged periods of time under increasing temperatures. Similarly, wetting events after long dry spells are associated with pulses in N gas fluxes. Both labile carbon accumulated during the drought and the intracellular compounds released by microbes in response to the increase in soil water potential are rapidly mineralized upon rewetting (Bergstermann et al. 2011; Fierer and Schimel 2003). As these events are brief, they typically contribute less to annual trace gas emissions than spring thaw events in northern ecosystems (Groffman et al. 2009). Finally, agricultural management practices such as irrigation, tillage, fertilization or harvest are pulsed events that expose previously occluded or newly added organic residues to mineralization, which can trigger large denitrification activities especially when they coincide with high soil water contents (Lucas et al. 2023a; Mutegi et al. 2010; Ostrom et al. 2021; Song et al. 2019).

During denitrification events the product stoichiometry can change quite drastically. Incubation studies have repeatedly shown that the $N_2O/(N_2O + N_2)$ product ratio decreases with time (Friedl et al. 2016; Robertson and Groffman 2007; Senbayram et al. 2019, 2022; Weier et al. 1993) due to delayed formation of N_2O reductase and decreasing inhibition of N_2O reductase with nitrate depletion.

Time is not only an important controlling factor of denitrification on short, event-related time scales. The denitrification potential of plant residues in soil also changes gradually with aging in soil. The water-extractable carbon fraction of POM is mainly fueling denitrification (Lashermes et al. 2022) and the water-extractable carbon content decreases with the number of leaching events (Surey et al. 2020).

Conceptual views and estimation methods of the anaerobic soil volume

Empirical relationship with bulk O_2 concentration

Bulk O_2 concentration has been shown to be a much better predictor for denitrification activity than water saturation alone (Burgin and Groffman 2012; Simojoki and Jaakkola 2000; Song et al. 2019), as oxygen availability is already an emergent property of oxygen supply imposed by the air-filled pore space and oxygen demand by autotrophic and heterotrophic respiration in soil. An early soil core incubation study observed escalating denitrification activity only at an O_2 content of 0.5% in macropores ($pO_2 = 0.5$ kPa) (Parkin and Tiedje 1984). The critical O_2 content for N_2O production amounted to 3% in another mesocosm study with sieved soil and coincided with a critical matric potential at which pores of 95–110 µm turn from air to water-filled (Du et al. 2023). Field studies have identified a critical O_2 content for N_2O emissions at a much higher level of 11–12% (Song et al. 2019; Wei et al. 2023) or observed no clear relationships at all for N_2O and a steep increase for N_2 at O_2 contents below 5% (Burgin and Groffman 2012). The critical O_2 content for the increase of N_2O concentration in soil and N_2O fluxes to the atmosphere can be different (Wei et al. 2023). This decoupling can be due to air trapping in soil pores, followed by sudden release when the matric potential reaches field capacity, rendering critical O_2 changes as the better predictor for N2O fluxes (Jarecke et al. 2016).

Under natural, non-flooded conditions the O_2 content in air-filled macropores is rarely below 15% (15 kPa) for long periods of time (Angert et al. 2015; Jarecke et al. 2016; Silver et al. 1999; Simojoki and Jaakkola 2000; Song et al. 2019; Wei et al. 2023). However, bulk O_2 measurements do not accurately capture O_2 concentrations at anaerobic microsites, which are typically located far from air-filled macropores and where most of the denitrification occurs

(Burgin et al. 2010). Distributed O_2 microsensor measurements showed very high variability at short spatial scales even in the absence of plant residues or other particulate organic matter (Rohe et al. 2021), with O_2 contents amounting to 15% in a macropore and 3% in the soil matrix a few mm away from it. These results highlight the limitations of estimating the anaerobic soil volume fraction via empirical relationships with bulk O_2 contents. Nevertheless, the anaerobic balloon is implemented as a function of O_2 content in many common nitrogen cycling models (see modeling section).

Relationship with microstructure – a sequence of paradigm shifts

Direct quantification of the anaerobic soil volume began with the development of O_2 microsensors some forty years ago (Sexstone et al. 1985) and was mainly focused on soil clods of different sizes (Højberg et al. 1994; Sierra and Renault 1995; Zausig et al. 1993). For decades, this pioneering work has shaped the common conceptual view of the anaerobic soil volume as being located in anoxic centers of wet soil aggregates (Fig. 1a) with soil structure represented merely as an assembly of aggregates (Ball 2013). Such aggregate assembly models have even been proposed as a basis for upscaling greenhouse gas fluxes from the scale of individual aggregates to the landscape scale (Ebrahimi and Or 2018).

A major step toward a more realistic picture of denitrification activity (red in Fig. 1) was the realization that denitrification may be decoupled from the total anoxic soil volume (gray in Fig. 1) and concentrated at the oxic-anoxic interfaces (Fig. 1b). This focus on interfaces first emerged in the studies of benthic sediments and flooded soils where concentration gradients and fluxes are mainly vertical and where the soil–water interface is the site of highest denitrification activity with little contribution from the underlying anoxic volume (Reddy et al. 1984). Modeling of denitrification in individual soil aggregates without nitrate limitation indicated that in unsaturated soil the oxic-anoxic interface is also a hotspot of microbial activity (Ebrahimi and Or 2015). At the interface, the aerobic microbial community intercepts oxygen diffusing into the aggregate, while the anaerobic community intercepts the carbon flux into the substrate-depleted aggregate surface resulting in the highest cell densities. These opposing gradients were later also experimentally confirmed by 2D micromodels (Borer et al. 2018). It is generally accepted that the coexistence of aerobic and anaerobic microsites in soil can promote coupled nitrification–denitrification (Braker and Conrad 2011; Friedl et al. 2021; Meyer et al. 2002; Nielsen et al. 1996; Pett-Ridge et al. 2006), i.e. that the nitrate produced by nitrification in the presence of oxygen is consumed nearby by denitrification in the absence of oxygen. We hypothesize that the greater the extent of such an oxic-anoxic interface, the
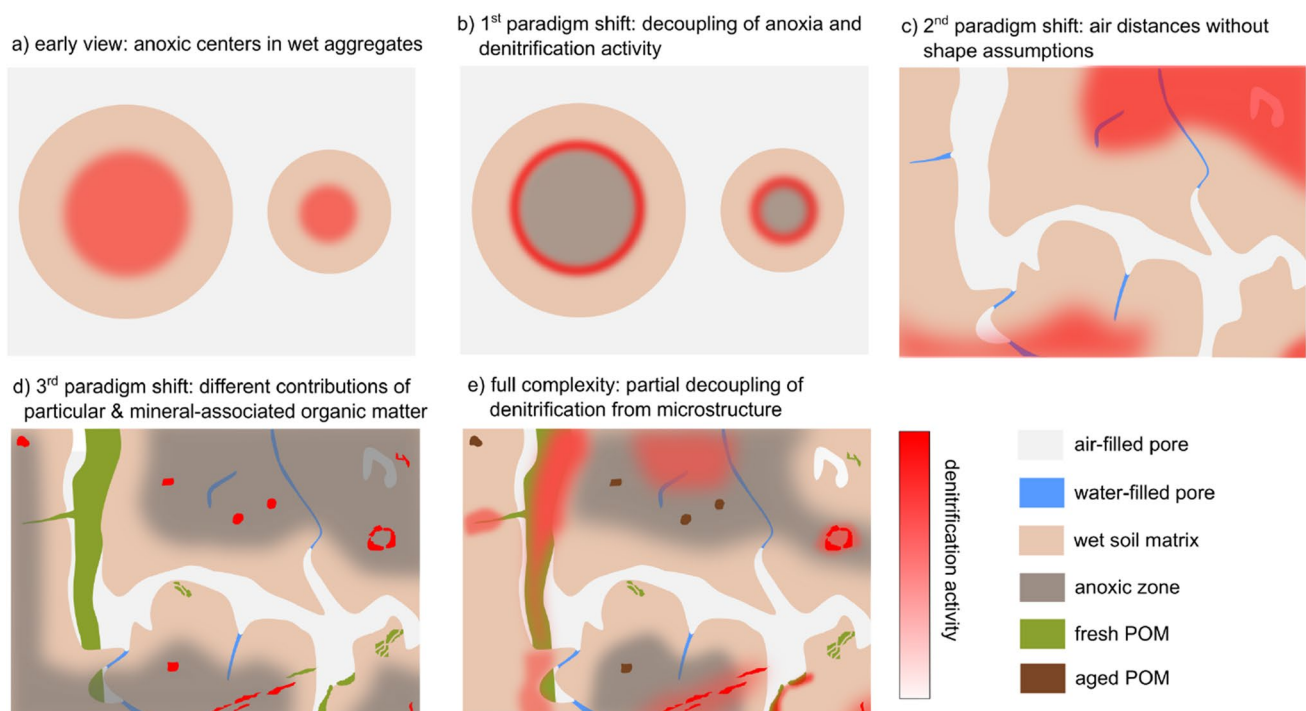

Fig. 1 Conceptual views of the changing paradigms in identifying sites of denitrification activity within soil microenvironments. Zones of denitrification activity (red) may decouple from anoxic zones (gray) in soil

greater the opportunities for nitrate transport and, hence, for coupled nitrification–denitrification. However, to our knowledge, the approach of quantifying the size of the oxic-anoxic interfacial area (or volume of the hypoxic fringe) and to relating it to denitrification activity has not yet been applied to intact soils.

The second major conceptual improvement came with the paradigm shift from the focus on individual aggregates of different sizes (Fig. 1a-b) to the distribution of distances from air-filled pores in the soil matrix (Fig. 1c). The old paradigm relied on critical sizes of convex or even perfectly spherical aggregates for the formation of anoxic centers under given boundary conditions, whereas the new paradigm did make no assumptions about the shape of the physical domain. Both paradigms state that the local oxygen availability depends on the diffusion constraints of dissolved oxygen through the wet soil matrix. However, ignoring the intact pore structure and dissecting the soil into artificial fragments is a questionable simplification of reality (Vogel et al. 2022) that may lead to drastic underestimation of denitrification activity. We would like to demonstrate this using the data from Rohe et al. (2021). Consider the soil sieved to 4 – 8 mm, repacked to 1.3 g/cm^3 and brought to an air content of 10%, for which the average air distance in the soil matrix is 0.99 mm (Fig. 2a). If the critical distance to air-filled pores, beyond which the wet soil matrix becomes anoxic is set at 1 mm, the anaerobic soil volume fraction in this soil is 40% (Fig. 2 b,e). Consider breaking the soil

into fragments, for the purpose of studying them in isolation according to the paradigms of Figs. 1a and 1b. The hypothetical fragmentation along the failure zones is shown on Fig. 2(c). Such destruction of the soil structure will lead to two simultaneous radical changes. First, the pore water in pre-existing "inter-aggregate" pores will be drained, and second, distances from the soil matrix to the air-filled pores will be greatly reduced (Fig. 2e). That is, in the intact case, the soil matrix far from air-filled pores extends over several fragments, but once the fragments are separated, it is only their individual sizes that determine the distances from the air-filled pores. The draining of the "inter-aggregate" pores alone will already reduce the average air distance and the anaerobic soil volume fraction to 0.55 mm and 16%, respectively, while the fragmentation will further reduce it to 0.45 mm and 11%. This fourfold reduction of the anaerobic soil volume fraction is even accompanied by an increase in water saturation, which is now 100% WFPS in the wet aggregates versus approx. 80% WFPS in the repacked soil.

The paradigm shift to air distances was facilitated by the technical advancement from needle-type microsensors to planar optodes in order to study oxygen distribution in intact or repacked soils under different environmental conditions. This allowed direct estimation of the anaerobic soil volume within areas of 10—100 cm^2. This approach has been used to study, among other things, oxygen leakage by rice roots into an otherwise anoxic, flooded paddy soil (Larsen et al. 2015), oxygen depletion around decomposing plant residues
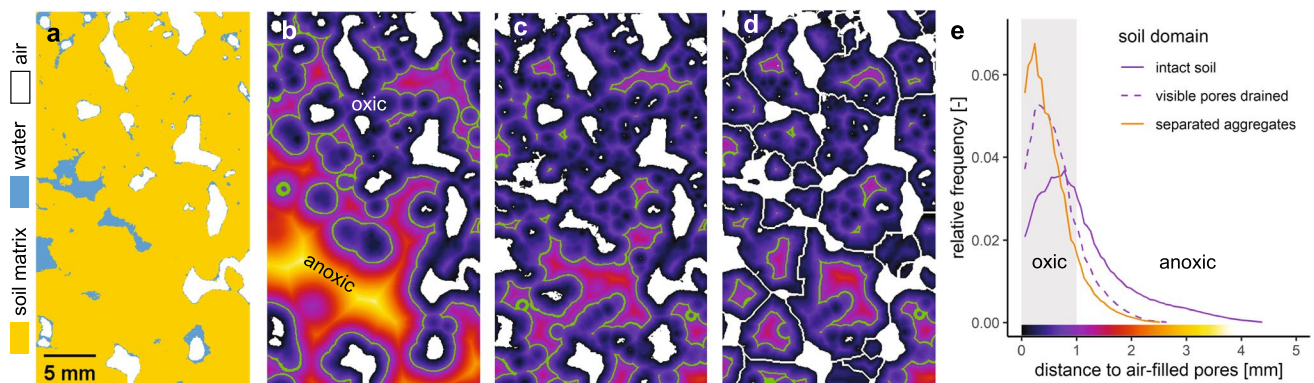

Fig. 2 Illustration of changes in distances to air-filled pores resulting from the hypothetical fragmentation of the intact soil matrix into a collection of "aggregates": (a) 2D slice of an X-ray CT scan of a soil sieved to 4–8 mm, repacked to 1.3 g/cm^3 and brought to an air content of 0.10 (approx. 80% WFPS) (Rohe et al. 2021). Image is segmented into water-filled soil matrix (yellow), air-filled pores (white), and water-filled pores (blue). (b) Distances to air-filled pores and the hypothetical anaerobic soil volume for the same slice, assuming a critical air distance of 1 mm. Color legend for distance sizes is included in e. (c) Distances to air-filled pores and the hypothetical anaerobic soil volume for the same slice when the water-filled pores are drained (assuming the same critical air distance of 1 mm). Color legend for distance sizes is included in e. (d) Distances to air-filled pores and the hypothetical anaerobic soil volume for the same slice when the aggregates are separated and thus their boundaries are set to air (assuming the same critical air distance of 1 mm). Color legend for distance sizes is included in e. e) Frequency distribution of the distances to air-filled pores in the soil matrix for (i) the original scenario depicted in b, i.e., the intact soil matrix with an air content of 0.10, (ii) the hypothetical fragmentation scenario where the aggregates are not yet formally separated but the water in pre-existing inter-aggregate pores is already drained, increasing the air content to 0.15, and (iii) the hypothetical fragmentation scenario depicted in d where both the aggregates are formally separated and the water in pre-existing inter-aggregate pores is drained and the air content in the aggregates is zero

in soils of contrasting pore structures (Kravchenko et al. 2017), the expansion of anoxia around pig manure placed in the soil in different spatial configurations (Zhu et al. 2015) or the relationship between the anaerobic soil volume an bulk oxygen contents in repacked soils of different carbon content (Keiluweit et al. 2018).

Direct measurements of the anaerobic soil volume with planar optodes have several drawbacks. The sampled areas are rather small, pore configurations and diffusion patterns along the sample walls are somewhat artificial, and a direct visualization of water-filled and air-filled pores is not possible. All of these shortcomings can by and large be overcome by X-ray tomography, which has therefore recently begun to play a more prominent role in denitrification studies (Kravchenko et al. 2018b; Lucas et al. 2023a; Ortega-Ramírez et al. 2023; Porre et al. 2016; Rabot et al. 2015; Rohe et al. 2021; Schlüter et al. 2019). The main drawback is that a direct estimation of the anaerobic soil volume is not possible and has to be done as a combination of both techniques (Kravchenko et al. 2017) or has to be replaced by a correlation analysis between N-gas fluxes and air distance metrics. A simplified approach is to compute the shortest distances to air-filled pores for all voxels within the wet soil matrix. Variations of this approach exist, e.g., where isolated air pockets without connection to the headspace are ignored for distance calculations (Rohe et al. 2021), or where simple Euclidean distances are replaced by geodesic distances around obstacles (Ortega-Ramírez et al. 2023). A histogram of these air distances can then be computed and examined for the entire soil matrix. Furthermore, the soil matrix can be segmented at a critical air distance into hypothetically oxic and anoxic fractions at shorter and longer distances, respectively. This paradigm of identifying denitrification activity patches is illustrated in Fig. 1(c). Implementation of this approach requires a sensitivity analysis, in which a series of air distance thresholds are evaluated to determine the critical distance at which the calculated potential anaerobic volume best correlates with measured denitrification activity. For repacked soils of two different carbon contents without visible plant residues this critical air distance was 5 mm, resulting in anaerobic soil volume fractions of < 0.01 up to 0.8 (1 being the entire mesocosm) in the WPFS range of 65 – 88%. (Rohe et al. 2021). Such a large variation in the anaerobic soil volume fraction was induced by the somewhat artificial, layered pore structure in repacked soils. This anaerobic soil volume fraction was a good proxy for oxygen supply, better than WFPS or relative gas diffusivity, and together with CO_2 emissions as a proxy for oxygen demand, predicted $N_2O + N_2$ emissions quite well ($R^2 = 0.83$). The distance threshold was found to be much shorter, as low as 0.18 mm in intact soil cores under several bioenergy cropping systems (Kravchenko et al. 2018b). The resulting anaerobic soil volume fraction was in the range of

0.4—0.9 for water saturations of 71 – 82% WFPS and was a good predictor of net N_2O emissions from bacterial denitrification ($R^2 = 0.57$). The much shorter distance threshold (5.00 vs. 0.18 mm) might have been due to the plant litter and fresh roots that start to decompose in the intact soils after sampling and thereby act as denitrification hotspots and induce much higher O_2 consumption rates locally.

The third and most recent paradigm shift accounts for the very different contributions of particulate and mineral-associated organic matter (MAOM) to denitrification in cultivated soils (Rummel et al. 2020; Surey et al. 2021). POM and/or water-soluble organic C are better proxies for bioavailability than soil organic matter (Lacroix et al. 2023) and should be evaluated separately to improve predictions of denitrification activity. This approach is illustrated in the conceptual figure (Fig. 1d) by mapping POM in the soil matrix and concentrating all denitrification activity in POM located beyond a given critical air distance. The average distance of POM to air-filled pores predicted N_2O emissions from intact cultivated soils incubated at -31.6 hPa ($> 60\%$ WFPS) remarkably well, with $R^2 > 0.75$ throughout the entire incubation period (Ortega-Ramírez et al. 2023). The explained variability of this single predictor, which combines both oxygen supply and demand in a single number, was much higher than with POM volume fraction or air-filled porosity alone. Thus, it is not the total POM amount, but rather its degree of occlusion in the wet matrix that is important for denitrification activity (Fig. 1d). A recent mesocosm study indeed indicated that distinguishing between this occluded POM in the soil matrix and POM near or within pores is crucial; the former was a reliable predictor of denitrification ($N_2O + N_2$ fluxes), while the latter significantly correlated with aerobic respiration (Lucas et al. 2024). Additionally, this study highlighted that the anaerobic volume fraction served as a valid predictor of denitrification only when POM is evenly distributed throughout the soil matrix. This distribution was observed in an investigated grassland soil, but not in a cropland soil, where most roots and consequently POM were localized within macropores. The association between occluded POM beyond a certain distance from air-filled pores and $N_2O + N_2$ fluxes or N_2O fluxes was very high across both land uses ($R^2 = 0.79$ and $R^2 = 0.90$ respectively). Both microstructure predictors, i.e. the anaerobic volume fraction in the soil matrix (Fig. 1c) and the air distance to POM (Fig. 1d), performed equally well (R^2 within a range of $0.5 – 0.6$) in predicting field $N_2O + N_2$ fluxes in soils under maize and sorghum cropping systems across fertilization and precipitation events (Lucas et al. 2023a). The critical air distance threshold was < 1 mm for both crops, resulting in variable anaerobic soil volume fractions of $< 0.01 – 0.24$ during a season. However, the same study also showed that the air distance based metrics were poor predictors of denitrification activity in switchgrass

cropping systems, where they were outperformed by root volume as the single best predictor ($R^2 = 0.44$). Oxygen consumption in the rhizosphere around the massive root systems of this perennial N-fixing plant appeared to be more important in promoting denitrification activity. Fresh, hydrophilic POM can absorb large amounts of water, and due to this sponge effect, can induce denitrification, even when it resides in air-filled macropores (Kim et al. 2020; Kravchenko et al. 2017). Indeed, the formation of anoxic microsites may be driven more by the POM-induced oxygen demand than by the oxygen supply imposed by soil texture (Lacroix et al. 2022). Such a scenario in which denitrification activity is mainly (but not exclusively) concentrated in POM, and in which denitrification activity is therefore partially decoupled from air-distances, is shown in Fig. 1e. We suspect that this is closest to the full complexity of the natural soil microenvironment, but it also illustrates why microstructure-based modeling approaches can easily fail in predicting denitrification activity.
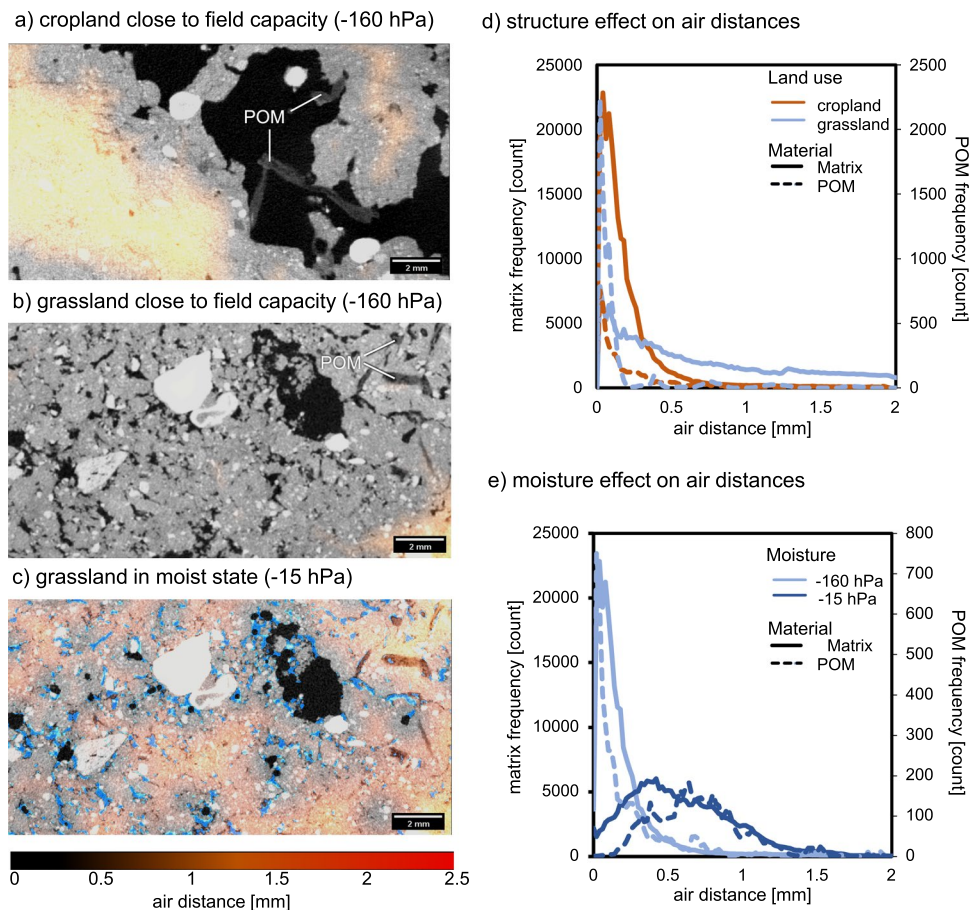
Another reason for this decoupling is the quality of POM. Soil-aged POM has reached on average two times greater air distances than fresh fibrous POM (Fig. 1e) due to fragmentation and soil structure turnover (Schlüter et al. 2022). However, its contribution to denitrification activity may be low due to losses of labile C by prolonged decomposition and potentially repeated leaching events (Surey et al. 2020). The separation of POM into different classes based on shape and texture has become more common (Leuther et al. 2022; Schlüter et al. 2022), but its full potential to refine predictions of denitrification potential has not yet been realized.

Case study: Air distances as a function of land use and soil moisture

This case study demonstrates that land use and soil moisture can have a drastic effect on the air distances in the soil matrix and the disconnection of POM from air supply. To illustrate commonly observed air distance values in topsoils and to compare them with estimated distance thresholds for the onset of anoxia (Sect. 3.4), we consider an intact soil structure from two contrasting land uses, a plowed arable soil (Fig. 3a) and a no-till grassland (Fig. 3b). We measured air distance values in them and estimated distance thresholds for the onset of anoxia. The internal structure of the samples was visualized by X-ray CT scans with a resolution of 20 μm. The local density is shown in gray tones from pores (dark) to mineral grains (bright). In addition, the Euclidean distance to the closest air-filled pore is shown with a color

Fig. 3 Case study of the factors controlling the anaerobic soil volume. The microstructure is shown here with 2D slices from X-ray CT scans of a) cropland and b) grassland soils, adjusted to a matric potential around field capacity (-160 hPa). The cropland is denser (1.3 g cm-3) and has a lower soil organic matter content (12 g kg-1) than the grassland (1.0 g cm-3, 39.5 g kg-1) (c) The hypothetical distribution of water (blue) in the grassland soil under very wet conditions of hm = -15 hPa. d) Air distances in the matrix and in POM for the two soils at field capacity. e) Air distances in the matrix and in the POM of the grassland soil for both matric potentials

a) cropland close to field capacity (-160 hPa)

b) grassland close to field capacity (-160 hPa)

c) grassland in moist state (-15 hPa)

d) structure effect on air distances

e) moisture effect on air distances

scale. We assumed that all unresolved pores in the images were water-filled, while all visible pores were air-filled. By relating capillarity to pore diameter via the Young–Laplace law for the given image resolution, this assumption would correspond to the soil matric potential around field capacity at -160 hPa; a common state for these soils at which denitrification is expected to occur. In addition, the grassland was artificially adjusted to a higher matrix potential (-15 hPa) by filling all pores smaller than 200 μm with water using a pore size opening (Fig. 3c); a condition that could be expected after a heavy rainfall event. Figures 3d and 3e illustrate the effect of structure and moisture on the frequency distribution of air distances for all soil voxels and additionally only for the locations of the POM.

In comparison, the grassland soil has a lower bulk density (1.0 g cm^{-3}) and a higher soil organic matter content (39.5 g kg^{-1}) than the cropland soil (1.3 g cm^{-3}, 12 g kg^{-1}), and the visible pores are more evenly distributed (Fig. 3b) than in the cropland soil (Fig. 3a). As a result, the average distances to air-filled pores in the soil matrix of the two soils are very different with 0.20 mm and 0.84 mm for the grassland and the cropland, respectively. In the grassland, distances from air-filled pores into the soil matrix hardly ever exceed 0.6 mm due to the disperse distribution of visible pores, whereas in the cropland soil a substantial part of the soil matrix is more than 0.6 mm away from the air-filled pores. POM resides in much closer vicinity to air-filled pores (Fig. 3b), most of it less than 0.4 mm, because it is located in biopores and decomposition creates a lot of inherent porosity (Schlüter et al. 2022). POM is more thoroughly mixed into the soil under grassland, with higher average air distances in the soil matrix (0.25 mm) than under the cropland soil (0.15 mm), despite the lower bulk density. When the soil is wetted to a matric potential of $h_m = -15$ hPa, i.e. by assuming that all pores smaller than 200 μm are filled with water (Fig. 3c), the average air distance in the soil matrix increases substantially to 0.59 mm in the grassland soil (Fig. 3d). The average air distance of the POM even increases beyond that of the matrix (to 0.70 mm), because many fine roots are contained in pores smaller than 200 μm.

The reported values are put into perspective below by comparing them to critical distance thresholds for the onset of anoxia derived from an extensive literature review.

Critical air distances for the formation of anoxia – a meta-analysis

As mentioned in the previous sections, the variability in critical air distances leading to the formation of anoxia and in the resulting anaerobic soil volumes can be enormous. They are most likely controlled by soil microstructure and by environmental factors that drive oxygen consumption or

replenishment in one way or another. To assess this variability and its drivers, we conducted a meta-analysis of a total of 89 data sets from 27 experimental studies. The studies spanned a range of experimental tools, with 16 using microsensors, six using planar optodes, and five using X-ray CT, and a range of domains including wet soil aggregates, biofilms, benthic sediments, flooded soils and intact upland soils. Critical air distances leading to formation of anoxia were either determined by a series of point measurements (microsensors), derived visually (planar optodes), or estimated indirectly from correlations between denitrification rates and air distance metrics (X-ray CT). The dataset and method description are included in the Supporting information (Dataset S1, Section S1).

The soil domains were categorized into three classes depending on whether distance thresholds were determined i) directly around labile carbon sources, e.g. biofilms, fresh leaves or manure, ii) in sieved soils without visible plant residues, e.g. single aggregates, repacked soils or iii) in soils with labile carbon, e.g. intact soil or soil mixed with POM
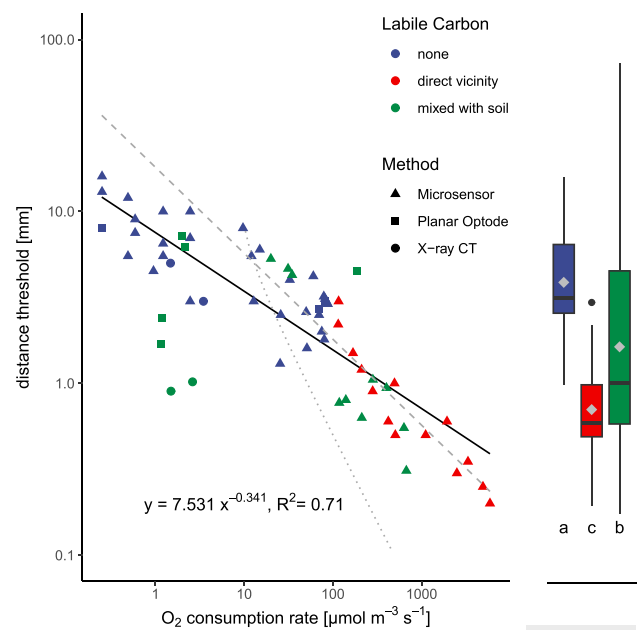

Fig. 4 Relationship between critical air distance for the formation of anoxia as a function of O_2 consumption rate derived from a meta-analysis of 27 experimental studies. Of the 89 datasets included in the meta-analysis, 22 did not have O_2 consumption rates. The black line represents a fitted power-law relationship with the parameters given in the figure. The gray dashed line represents the analytical solution for a plane with an external oxygen concentration of 21 kPa, for a detection limit for anoxia set to 0.1 kPa and a relative diffusion coefficient set to $D/D_0 = 0.001$. The dotted line shows the analytical solution for a spherical domain with a radius of 10 mm with the same settings. The box plots on the right show the distribution of critical air distances for different categories of whether and how labile carbon in soil was considered (gray diamond – arithmetic mean), including all 89 datasets. Differences are tested at a significance level of $p < 0.05$

(Fig. 4). The distance thresholds varied by two orders of magnitude and ranged from 0.18 to 73 mm. Shorter distances were difficult to resolve and larger distances were rare as anoxic regions would simply not form under well aerated conditions with large oxic margins. In soils without labile carbon, the mean critical air distance for the formation of anoxia amounted to 3.9 mm (median 3.2 mm). This distance was reduced significantly to 1.9 mm (median 0.9 mm) when labile carbon was mixed into the soil, and even further to 0.7 mm (median 0.6 mm) when measured directly in the vicinity of labile carbon, e.g. around fresh leaf residues or pig manure. The distance threshold exhibited a highly significant relationship with O_2 consumption rates ($R^2 = 0.71$) and followed a power-law relationship with the fitting parameters:

$$d_{anox} = 7.531 q^{-0.341}$$

with the distance threshold d_{anox} in mm and the O_2 consumption rate q in $\mu mol\, m^{-3} s^{-1}$. Analytical solutions for the critical air distance in a planar domain (dashed line),

$$d_{anox} = \sqrt{(c_0 - c_{lim})\frac{2D}{q}}$$

in a spherical domain (dotted line),

$$d_{anox} = r_0 - \sqrt{r_0^2 - (c_0 - c_{lim})\frac{6D}{q}}$$

are also shown in Fig. 4, with a sphere radius, r_0, of 0.01 m and an assumed external oxygen concentration in the liquid, c_0, of 285 $\mu mol\, L^{-1}$ and assumed detection limit for anoxia, c_{lim}, of 13.5 $\mu mol\, L^{-1}$. This corresponds to partial pressures of $p_0 = 21 kPa$ and $p_{lim} = 1 kPa$ through

$$c = H\frac{p}{RT}$$

with the Henry constant H of 3.2×10^{-2}, temperature T in K and the universal gas constant R of 8.314 $J\, mol^{-1} K^{-1}$. The diffusion coefficient D of 6×10^{-10} m^2 s^{-1} was fitted manually in order to align d_{anox} with the measured data. The fitted D is in the range of measured or estimated diffusion coefficients in the studies used for this meta-study ($2 \times 10^{-12} - 9 \times 10^{-9} m^2 s^{-1}$). It is smaller than the diffusion coefficient of oxygen in water ($D_w = 1.67 \times 10^{-9}$ m^2 s^{-1}) due to diffusion restrictions imposed by the solid matrix. For the common Millington-type function (Millington 1959):

$$\frac{D}{D_w} = \theta^{4/3}$$

this reduction would occur at a volumetric water content of 0.46, a reasonable value for incubation studies that were adjusted to near saturation. The fitted, critical diffusion

coefficient in water corresponds to a relative diffusion coefficient, D/D_0, of 0.001 in air (with oxygen diffusion in air of $D_0 = 1.98 \times 10^{-5} m^2\, s^{-1}$ and a dimensionless Henry constant of 3.2×10^{-2}). It is smaller than the previously reported critical range of relative gas diffusivity, D/D_0, of $0.005 - 0.01$ (Balaine et al. 2013; Chamindu Deepagoda et al. 2019; Li et al. 2021; Owens et al. 2017; Rousset et al. 2020) derived from macroscopic N-gas release into the headspace. The discrepancy suggests that some of the assumptions underlying the analytical solutions are incorrect, such as uniform spatial distribution of the O_2 consumption rate q and the domain boundary as the only source of oxygen. The measured data agrees better with the analytical solution of a planar domain than with that of a spherical domain. There was measurable denitrification activity for $q < 10$ μmol m^{-3} s^{-1}, although the analytical solution for rather large spherical aggregates (∅ 20 mm) predicts no anaerobiosis at all at this moderate microbial activity.

Since O_2 consumption rates are not routinely measured in denitrification studies, robust relationships with more readily available soil properties need to be identified. For this meta-study, a selected set of soil properties was available for almost all data points: soil organic matter content SOC in g C kg^{-1}, temperature T in °C, external oxygen content pO$_2$ in kPa and matric potential h$_m$ in –hPa (i.e. high suction counting positive). Note that soil moisture in the very wet range is more easily adjusted by matric potential or varying water tables, so this information was often reported rather than water saturation in %. Highly significant power-law relationships were identified in the following form:

$$d_{anox} = a\, SOC^b\, T^c\, pO_2^{\ d}\, h_m^{\ e}$$

The explained variability with basic soil properties was reduced to $R^2 = 0.269$ (Table 1), when all data points were considered, including those studies where labile carbon was

Table 1 Exponents of the empirical power-law relationships between the critical air distance threshold for the formation of anoxia (d$_{anox}$) and several bulk soil properties

parameter	data without labile carbon ($n=36$)	Data with labile carbon ($n=25$)	All data ($n=61$)
a (intercept)	exp(-9.110)***	exp(4.413)	exp(0.739)
b (SOC effect)	-0.195*	-0.689	-0.514***
c (T effect)	0.710*	-0.929*	-0.067
d (O$_2$ effect)	2.869***	-0.118	0.582*
e (water effect)	0.145*	0.245'	0.186
Adjusted R^2	0.717	0.347	0.269

The data from a literature review is grouped according to whether soil contained labile carbon in the experimental setup. A significant effect of a given bulk property on **d$_{anox}$** is reported as *** $p < 0.001$, ** $p < 0.01$, * $p < 0.05$, ' $p < 0.1$

added to soil. Apparently, the presence of labile carbon is not reflected in any of the basic soil properties. When the model was fitted separately for data points with and without labile carbon, the explained variability increased to $R^2 = 0.347$ and $R^2 = 0.717$, respectively. Moreover, the relative importance of the explanatory variables changes drastically with the samples considered. In soils without intense microbial hotspots all explanatory variables have a significant effect on the distance threshold, with pO_2 having a superior role. In soils with microbial hotspots, all soil properties become irrelevant, except for a slight trend with matric potential, and only incubation temperature modulates the anoxic zone around hotspots. For all data combined, only SOC as a proxy for oxygen demand and the external pO_2 as a proxy for oxygen supply had a significant effect on the distance threshold. The signs of the estimated parameters were mostly consistent with their hypothesized effects on the distance threshold, e.g., the threshold was increased by lower SOC content, lower temperature, higher external O_2 content, and higher suction. Interaction effects were not considered in this meta-analysis. For a typical incubation scenario, where soil samples with 10 g C kg-1 are brought to a matric potential of -10 hPa and incubated at 20 °C and at ambient oxygen conditions (21 kPa), the predicted distance thresholds would be 5.11 mm, 1.28 mm and 4.73 mm for soils without microbial hotspots, with microbial hotspots, and all soils combined, respectively.

With the new conceptual model for denitrification activity based on microscale properties that we present at the end, this distance information can be used directly. To make such empirical relationships more general, they should be extended to include other potentially important controlling factors such as clay content, mineral nitrogen content and/or pH.

Oxic-Anoxic denitrification ratio – a meta-analysis

The distance threshold for the formation of anoxia is a useful concept based on detailed pore structure information. The question remains whether there might be so far unnoticed, potentially useful predictors of the anaerobic soil volume which could be derived directly from measured gas fluxes without the need to analyze the microscopic structure; as such a microstructure analysis is rarely done in denitrification studies. We conducted another meta-analysis with focus on those gas fluxes, in which we reviewed experimentally determined anaerobic soil volume fractions from 17 studies with a total of 83 datasets. We collected a long list of meta-information, following and extending the standard reporting framework for denitrification research (Almaraz et al. 2020). The dataset and method description is added to the Supporting information (Dataset S2, Section S2).

This complementary approach to experimentally determine the anaerobic soil volume without microscale

information was proposed about forty years ago (Parkin and Tiedje 1984). The ratio of denitrification activity in soil incubated at ambient, or non-zero oxygen concentration to that of the same soil incubated in an O_2 free atmosphere should give a good approximation of how much anaerobiosis developed in microsites during the oxic incubation stage (Parkin and Tiedje 1984; Rohe et al. 2021). The validity of this approach depends on some rather strong assumptions. i) N_2O in the oxic treatment should only originate from denitrification, and not from nitrification. Otherwise, apparent anaerobic soil volume fractions > 1 are possible. ii) Aerobic denitrification (Yang et al. 2020) is absent, otherwise apparent anaerobic soil volume fractions would be overestimated. iii) Oxygen consumption and potential denitrification activity should be uniformly distributed over the soil volume. Otherwise, the inference of volumes from rates is questionable. iv) Rate comparisons should be done for a steady state situation in both incubation stages. Otherwise, rate limitations by availability of labile carbon or N species in one of the stages may bias the ratio (see Method section S2).

The dataset covered the entire possible range of apparent anaerobic soil volume fractions (seven data points > 1 were excluded from the analyses) with an average of 0.35 (Fig. 5). This wide range is an asset for identifying controlling factors of the anaerobiosis formed under oxic conditions. The ratio of denitrification rates (oxic over anoxic) did not correlate well with the ratio of respiration rates
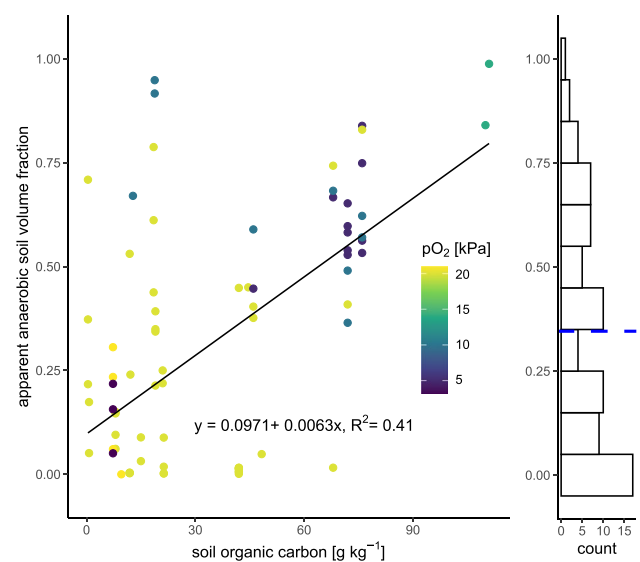

Fig. 5 Apparent anaerobic soil volume fraction estimated from the ratio of denitrification rates ($N_2O + N_2$) of oxic incubation to anoxic incubation. The marginal distribution (right) shows the spread across the entire range and the mean (blue dotted line). The scatter plot shows the relationship and the linear model with soil organic carbon content as the single best predictor. The color scale shows the external partial pressure of oxygen (pO_2). Most of the reported oxic incubations were conducted at ambient or very low hypoxic conditions

Table 2 Linear regression results of the apparent anaerobic soil volume fraction estimated from the ratio of denitrification rates ($N_2O + N_2$) of oxic incubation over anoxic incubation with several input parameters

regression	input variable	Direction	adjusted R2	p-value	degrees of freedom	min	median	max	unit
simple	pH	↔	-0.02	0.772	51	4.1	5.9	8.5	-
	C:N	↔	-0.01	0.391	64	6	10	65	-
	clay	↔	0.03	0.341	49	2	20	37	%
	WFPS	↑	0.07	0.019	72	0.43	0.64	1	-
	N_{min}	↓	0.09	0.007	67	0.2	35.8	241.6	mg N kg-1
	q_{anox}/q_{ox}	↑	0.14	0.006	47	0.23	0.43	1.82	-
	N_{tot}	↑	0.17	<0.001	64	0.2	2.2	9.8	mg N kg^{-1}
	bulk density	↓	0.26	0.000	62	0.41	1.11	1.5	g cm^{-3}
	T	↓	0.29	<0.001	56	6	20	25	°C
	pO_2	↓	0.31	<0.001	74	3	20	21	kPa
	SOC	↑	0.41	<0.001	72	0.4	21.3	111	g C kg^{-1}
multiple	$SOC + pO_2 + WFPS$		0.31	0.006	66				
	all with $p < 0.05$		0.77	0.008	17				

Positive (↑), negative (↓) and indifferent (↔) coefficients for simple regressions are assigned according to p-values ($p < 0.05$). The degrees of freedom vary with missing input information from the literature review and with the number of input variables of the linear model. The minimum, median, maximum and unit of all input variables are also reported

(anoxic over oxic) (Table 2, adjusted R^2: 0.14) for the subset of data points for which all gases (CO_2, N_2O, N_2) were measured. This is surprising as a switch to anoxic conditions should increase the volume in which denitrification occurs in the presence of carbon substrates and nitrate and at the same time reduce microbial activity in previously oxic regions. In addition, we have examined nine bulk soil properties (soil organic carbon (SOC) content, total nitrogen content, C:N ratio, mineral nitrogen content ($NO_3^- + NH_4^+$), pH, clay content, bulk density, water saturation, oxygen concentration during oxic incubation, temperature) for their individual and combined effect on the apparent anaerobic soil volume fraction. Not all of them were reported for all datasets, which reduces the subset of included data points, especially for multiple regressions (Table 2). SOC content was the single best predictor of the apparent anaerobic soil volume fraction (Fig. 5, Table 2) with a moderate adjusted $R^2 = 0.41$. This is consistent with the most significant effect of SOC on the critical distance for anoxia formation (Table 1, all data). The explained variability did not increase further when SOC content was combined with water saturation (i.e. WFPS) and external oxygen concentration (pO_2). This somewhat surprising finding may have three possible explanations. First, the WFPS and pO_2 ranges may simply have been too small or fragmented to make a difference. For instance, most of the incubations were performed at ambient conditions ($pO_2 \approx 20$ kPa) and only a few at hypoxic conditions ($pO_2 < 10$ kPa), with hardly any in the range between (Fig. 5). Second, the analysis of critical distances indicated that the water and oxygen effect are most important

for soils without plant residues and other POM (Table 1, soils without labile carbon). In other words, the physical diffusion constraints are more relevant for denitrification activity in the "cold" soil matrix, whereas denitrification activity in hotspots formed on POM is partially decoupled from bulk water and oxygen contents. Third, the added information content of pO_2 in the multiple regression with SOC is low, despite a rather high adjusted $R^2 = 0.31$ for single regression, because on average soils with higher SOC happened to be incubated at lower external oxygen concentration. Since the amount of plant residues or other proxies for labile carbon were typically not reported (too few entries for DOC in Data S2), SOC was the input variable that best approximated its abundance, but with a large share of unexplained variability. The low predictive power of total and mineral nitrogen content and C:N ratio could be due to the fact that denitrification is not nitrogen-limited in most incubation studies, either because it was added in large amounts at the beginning or because the late N-limited stages are excluded from the calculation (see Methods S2). Clay content was irrelevant for the anaerobic soil volume most likely because mesocosms were often saturated beyond natural, texture-dependent drainage conditions that would occur around field capacity. Presumably, temperature did not deviate enough from standard laboratory conditions in a sufficient number of incubations to have an effect, which may explain the somewhat artificial negative correlation of the anaerobic soil volume fraction with temperature. The negative correlation of the anaerobic soil volume fraction with bulk density reflects the fact that in the dataset higher bulk densities are correlated with

lower SOC contents. The pH effect on the anaerobic soil volume fraction and thus total denitrification is perhaps much smaller than its effect on denitrification completeness. The large gain in explained variability through the combination of all significant input parameters cannot be explained by a combination of complementary information, but is caused by the reduction to a small number of consistent data points in which all properties were reported (Table 2, Adjusted R^2: 0.77, $n = 17$).

Modeling concepts of soil anaerobicity and denitrification

Several models with varying complexity have been developed to simulate denitrification with different degrees of spatial resolution and with or without explicit consideration of soil anaerobicity. This review is limited exclusively to models of the former type, i.e., in addition to aerobic and anaerobic microbial growth and the production of gaseous nitrogen species and CO_2, soil physical processes including water distribution in the matrix and oxygen diffusion are explicitly simulated. In the following, pore-scale models are distinguished from upscaled, somewhat simplified, one-dimensional soil profile-scale models and other approaches. Finally, a new upscaled model based on microstructural information is proposed.

Aggregate and pore scale models

The investigation of anaerobic soil volume fraction within soil aggregates was pioneered by Currie (1961), who distinguished between macro-diffusion of oxygen along the vertical soil depth dimension and micro-diffusion within aggregates of structured soils at a given depth. This concept of diffusion was extended to diffusion within and between aggregates and applied to log-normally distributed aggregate size distributions (Smith 1980). This approach was later applied to modeling of denitrification at the soil profile scale (Arah and Smith 1989). Extending these models to scenarios involving multiple aggregates within 2D models, revealed a possible phenomenon in which aggregates provide shelter to each other based on their relative positions (Bocking and Blyth 2018). As a result, certain aggregates receive less oxygen than their neighbors.

The problems introduced by conceptualizing soil structure as aggregate assemblies were discussed in Sect. 3.2 in conjunction with the paradigm shift to air distances in a continuous soil domain (Fig. 1a,c). This conceptual shift also occurred in denitrification modeling with an alternative mechanistic approach emphasizing radial diffusion from air-filled pores into the surrounding bulk soil (Rijtema and Kroes 1991). Like the aggregate model, the pore model accounts for micro-diffusion from aerated pores into the bulk soil and can be combined with macro-diffusion along the vertical soil profile. A direct comparison showed that each approach has its inherent strengths and weaknesses, with no clear preference for one model over the other (Arah and Vinten 1995). For both approaches, statistical regressions could be derived between the modeled anaerobic soil volume fraction and soil texture, moisture content, metabolic activity and oxygen concentration. Thus, both the spherical aggregate and cylindrical pore models expressed as a simple proxy function (rather than comprehensive explicit models of oxygen diffusion and consumption) could be used in larger scale models. The cylindrical pore model (Rijtema and Kroes 1991) was later extended to a more sophisticated representation of bundles of pore size classes based on water retention characteristics (Schurgers et al. 2006). Differences in the resulting anaerobic soil volume fractions between the two models occurred mainly at near-saturated conditions (80–90% WFPS) and were caused by the contribution of small pores to aeration of the surrounding soil matrix in pore classes model (Schurgers et al. 2006). The pore class model lends itself naturally to coupling with basic soil properties, because of the existence of pedo-transfer functions derived from large databases of soil hydraulic properties (Carsel and Parrish 1988; Schaap et al. 2001; Wösten et al. 1999).

A rather new approach of three-dimensional modeling anoxic microsites based on soil structure information has been introduced by Ebrahimi and Or (2015), who developed a 3D angular pore network model that complements the theoretical framework of anaerobiosis in soil aggregates (modeled after Currie (1961) and Smith (1980)). In addition to diffusive transport of water, carbon and nitrogen, microbial motility due to chemotaxis was also considered. This also shed new light on the role of carbon distribution within soil aggregates. For instance, in the absence of internal carbon, anaerobes become extinct, whereas in the absence of external carbon, both aerobes and anaerobes coexist, but aerobes shift toward the aggregate core, changing their spatial distribution (Ebrahimi and Or 2015).

Soil profile scale models

Although much process understanding has been achieved at the pore scale, the representation of denitrification at the soil profile scale needs to be coupled with models describing the dynamics of other relevant soil properties at this scale. Appropriate models at the soil profile scale are typically one-dimensional, dividing the soil into different layers along the vertical axis. They are based on the assumption of lateral

homogeneity in terms of effective system properties, such as bulk density, soil water content, or root density, are often measurable under field conditions. As reviewed by Heinen (2006), many models at this scale do not explicitly include a state variable for the anaerobic soil volume, but use proxies primarily related to soil water content. For instance, in early versions of the DNDC model, denitrification rates were controlled by a basic switch triggered by precipitation and soil moisture thresholds (Li et al. 1992). In the NGAS model embedded in larger DAYCENT model, denitrification is controlled by a functional relationship based on water content, respiration, and an index of gas diffusivity (Del Grosso et al. 2000). The impact of soil structure is implicitly included by accounting for a texture-dependent gas diffusivity index, assuming that a high clay content would lead to a high anaerobic volume at modest water contents, if respiration is high.

However, some models went a step further by considering vertical oxygen diffusion and explicitly formulating the anaerobic soil volume based on partial oxygen pressure (Kraus et al. 2015; Li et al. 2000; Zhang et al. 2022), (see Table 3 for an overview). Li et al. (2000) coined the term "anaerobic balloon" to emphasize the dynamic nature of aerobic-anaerobic portioning of the soil. This type of model incorporates 1D vertical macro-diffusion while accounting for microbial and fine root respiration as sink terms. The mathematical representations of the anaerobic soil volume in these models lack a physical mechanistic basis and are instead based on heuristic principles. However, this approach is easier to implement than explicit modeling of micro-diffusion of oxygen and consumption in soil aggregates or the pore space, which would require detailed information on a number of soil physico-chemical parameters and their spatial distribution and is also numerically challenging to solve.

The anaerobic soil volume fraction can be used as a process switch or scaling parameter. In the case of Coup, DNDC and LandscapeDNDC (Blagodatsky et al. 2011; Kraus et al. 2015; Norman et al. 2008), the anaerobic soil volume is additionally used to partition nitrogen and carbon species into aerobic and anaerobic fractions. For process rate calculations such as nitrification or denitrification, only the respective fraction of total NH_4^+ or NO_3^- within the aerobic or anaerobic part is considered in the Michaelis–Menten or other process descriptions.

Table 3 summarizes the empirical formulas for the calculation of the anaerobic soil volume V_a from the partial pressure of oxygen pO_2 or other state variables and soil properties. A graphical representation of the $V_a - pO_2$ relationship (Fig. 6) indicates a huge variability in V_a among the models at ambient conditions and also that not all models approach $V_a = 1$ at $pO_2 = 0$ kPa. We also tested how well some of these field-scale models (LandscapeDNDC, DNDC.vCan and COUP) were able to reproduce the apparent anaerobic soil volume fraction determined experimentally with the

measured total denitrification activity in a coupled oxic-anoxic mesocosm incubation introduced in Sect. 3.5. The mesocosm experiments were conducted for a combination of three soils (silt loam cropland and clayey grassland soil in Fig. 2 and sandy cropland soil) and four water saturations (60 -75% WFPS). The models were run with the soil properties and boundary conditions of the oxic stage of the mesocosm incubation. The full model comparison is available as Supporting information (Section S3). There was a large variability between the modeled anaerobic soil volume fractions among models irrespective of soil (COUP: 0.02 – 0.06; LandscapeDNDC: 0.12 – 0.20, DNDC.vCan: no anaerobicity during oxic stage), but none of them was close to the experimental values for all soils and saturations. Furthermore, the variation of the modeled anaerobic soil volume fraction with water saturation was quite small, so that none of the models captured the steep increase in the measured anaerobic soil volume fraction around 75% WFPS. Reasons for these poor model performances are discussed in Section S3.

Few one-dimensional soil profile models have directly adopted numerical and statistical data from three-dimensional soil structure models. For instance, Refsgaard et al. (1991) implemented an aggregate diffusion model (Currie 1961) into the vertical one-dimensional SHE model (Abbott et al. 1986). Riley and Matson (2000) used the statistical representation of anaerobic soil volume as calculated by Rijtema and Kroes (1991) and proposed by Arah and Vinten (1995). In this model called NLOSS, the calculation of anaerobic soil volume depends on oxygen concentration in air-filled pores (C), oxygen consumption rate (V), volumetric soil water content (θ), air-filled porosity (ε_a), and radius of typical air-filled pore at moisture tension $\psi(r_\psi)$ (Table 3). The ANIMO model has adapted the pore diffusion model by using the anaerobic soil volume fraction to scale denitrification and nitrification (Groenendijk et al. 2005). This concept was further developed in the SWAP-ANIMO model (Stolk et al. 2011) by introducing the notion of an immobile zone, representing the pore space within aggregates, and a mobile zone, representing the space between the aggregates. Similar to the DNDC concept of anaerobic soil volumes, nitrification takes place exclusively in the mobile zone, while denitrification occurs in the immobile zone.

A consistent physically based upscaling of the aforementioned three-dimensional pore model (Ebrahimi and Or 2015) to a one-dimensional soil profile model and even beyond was presented by the same authors (Ebrahimi and Or 2016; 2018). They developed analytically solvable functions for, e.g. respiration and denitrification activity based on the results of numerical pore-scale models, which were WWconvenient abstraction of the complex soil structure. This lumped parameter represents small scale heterogeneity in analytical or numerical models to simulate denitrification

Table 3 Empirical functions linking oxygen concentration in soil with the anaerobic soil volume fraction in some common profile scale models of denitrification

Model	Formula	Transport concept	Parameters	Publication
PnET-N-DNDC	$V_a = a\left(1 - \left(b\frac{p_{O_2}}{p_{O_2}^*}\right)\right)$	1D gaseous diffusion in the aerobic and anaerobic soil volume; hourly time step size, N-species and O_2 are exclusively considered in the gas or liquid base; different parametrization of N-species and O_2 diffusion $D_N^* = \theta_g^{1.95}\theta^{1.5}$ $D_{O_2}^* = \theta_g^{1.75}\theta^{1.25}$	Scaling parameters a and b determine lower and upper boundary of V_a; not provided in the publication. Default values are a=1, b=0.92	(Li et al. 2000)
LandscapeDNDC COUP	$V_a = e^{-\left(ap_{O_2}^b\right)}$	1D gaseous diffusion in the aerobic and anaerobic soil volume; hourly time step size, gas and liquid phase are considered assuming instantaneous equilibrium $D^* = \theta_g^{\frac{7}{3}}$	a=7, b=2 COUP: a=7.071 or 10; b=2	(Kraus et al. 2015) (Norman et al. 2008)
DNDC-Can	$V_a = 1 - \frac{Eh}{650}$ $Eh = 1000\left(a - bln\left(\frac{1}{C_{O2}+c}\right)\right)$	1D gaseous diffusion in the whole pore volume, hourly time step size, gas and liquid phase are considered assuming instantaneous equilibrium $D^* = \theta_g^{2.5}\left(\frac{\theta_g}{\theta_s}\right)^{1}$	Scaling parameters a, b and c not provided in publication, Default values are: a=0.816, b=0.0063, c=1e-50	(Li et al. 2012)
NLOSS	$V_a = exp\left(-ar_\psi^{-\alpha}V^{-\beta}C^\gamma\left[\theta_w + \chi\theta_g\right]^\delta\right)$	gas and liquid phase are considered assuming instantaneous equilibrium	$a=1.5e^{-6}$, $\alpha = 1.26$, $\beta = 0.6$, $\gamma = 0.6$, $\delta = 0.85$	(Riley and Matson 2000)
SWAP-ANIMO	$V_a = min\left(a, b\frac{\theta_w}{\phi}\right)$	1D simultaneous diffusion of liquid and gaseous phase (note: only the aerobic, mobile phase is subject to transport), daily time step size; gas and liquid phase are considered assuming instantaneous equilibrium $D^* = \theta_g^{\frac{4}{3}}$ $D_{w:g}^* = \alpha_R P_1 \theta_g^{p_2} D_{0,g} + \tau_w \theta_w D_{0,w}$	a=0.95, b=0.95 p_1, p_2 not provided in the publication	(Stolk et al. 2011)

V_a: anaerobic soil volume; D^*: relative diffusion coefficient; D_N^*: relative diffusion coefficient specific for N-species; $D_{O_2}^*$: relative diffusion coefficient specific for O_2; $D_{w:g}^*$: relative diffusion coefficient for simultaneous transport in the gas and liquid phase; p_{O_2}: partial pressure of O_2; $p_{O_2}^*$: reference partial pressure of O_2 in the atmosphere; θ_g: gas content; θ_w: water content; Eh: redox potential; r_ψ: radius of typical air-filled pore at moisture tension ψ; $\bar{V}$: oxygen consumption rate, ψ; $\bar{V}$: oxygen consumption rate; C: oxygen concentration in air-filled pores, χ: ratio between the molecular diffusivity of O2 in air and water equal to 10^4; ϕ: porosity; α_R: reciprocal of Bunsen's solubility coefficient, $D_{0,g}$: Diffusion coefficient in free air, $D_{0,w}$: Diffusion coefficient in free water, C_{O2}: concentration of O_2 in soil air
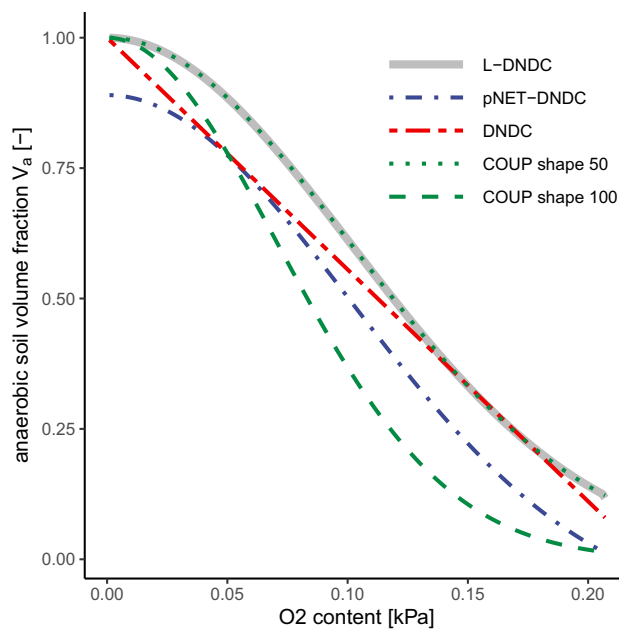
Fig. 6 Anaerobic soil volume fraction as a function of oxygen partial pressure. The dependencies from the following models are plotted: DNDC (Li et al. 1992); pNET-DNDC (Li et al. 2000); Landscape-DNDC (Kraus et al. 2015); COUP (Norman et al. 2008). Equations and parameter values are shown in Table 3. The two variants of the COUP model correspond to $a^b = 50$ and $a^b = 100$, respectively

under changing boundary conditions at the scale of soil profiles. In contrast, Sihi et al. (2020) directly used measurements to derive probabilistic distribution functions for soil carbon and soil water, to describe soil heterogeneity. They then applied a numerical model (DAMM-GHG) to a representative sample extracted from these probabilistic distribution functions and integrated the results.

While physical, mechanistic studies at the microscale have a long history, it's notable that the majority of commonly used one-dimensional soil profile models for field-scale research do not integrate these intricate mechanisms, although some have demonstrated their feasibility. This limited adoption is not surprising and can certainly be attributed to the complex regulation of denitrification as detailed in Sect. 3 and associated uncertainties in parameter determination, particularly if the model is to be universally applicable to different soil types. Moreover, no single approach has emerged as the superior choice, neither at the pore scale in three dimensions nor in the one-dimensional soil profile context. To streamline and improve these approaches, a clear strategy is needed in order to (i) identify the most salient microscale drivers of denitrification (as attempted in this review), (ii) translate these into proxies that are commensurate with parameters and state variables which are already implemented in denitrification models acting at the soil profile scale and (iii) establish empirical relationships

between them that are applicable to a wide range of soils and land uses.

The different factors relevant to local anaerobiosis, as discussed in Sect. 3, suggest the potential benefits of separating POM and MAOM in process models. Although the distinction in models has received limited attention so far, the studies by Ebrahimi and Or (2016) and Sihi et al. (2020) show promise in addressing this challenge by accounting for different POM distributions in the initial conditions of the pore network model or by explicitly considering POM in the measurements and initial formulation of probability distribution functions for soil carbon. In the next section, we will address the upscaling of another important micro-scale driver of denitrification activity to the soil profile scale, namely the air distances of the soil matrix in general and POM in particular.

The way forward: a 1.5-dimensional denitrification model based on microstructure

This review has provided considerable evidence that incorporating microstructural information into denitrification models is a promising way forward. In Sect. 3 it was found that the distance from the nearest air-filled pore and the availability of readily decomposable organic carbon in the soil matrix are the main controlling factors for denitrification. In the following we propose a 1.5 dimensional denitrification model based on this microstructural information (Fig. 7).

Current models operating at the continuum scale of a soil profile (Sect. 4) account for the very different diffusion coefficients of gases in air and water by representing the downward macro-diffusion of oxygen in air, the 1st dimension, and coupling it with lateral micro-diffusion of dissolved oxygen in simplified geometries like spherical aggregates or cylindrical pores, the 2nd dimension (Ebrahimi and Or 2016; Refsgaard et al. 1991; Riley and Matson 2000). The 1.5 dimensions arise from the fact that a lateral "half dimension" is not directly connected to the one below or above. We propose to generalize this behavior by dividing a soil core or soil profile into layers orthogonal to the vertical axis and determining the volume of the wet soil matrix at a given distance to the nearest air-filled pore, as well as the area of the interface between the adjacent volumes, and using them as weighting factors in the numerical discretization of the half dimension. In other words, the equally sized lateral nodes in the schematic (Fig. 7) have different volumes in the model and their connections have different surface areas. Knowledge of air-distance histograms obtained from X-ray CT scans of the corresponding soil layer can be incorporated into the model and can be used to more flexibly represent the geochemical gradients orthogonal to the air-filled pores. This is based on the assumption that all locations in the soil
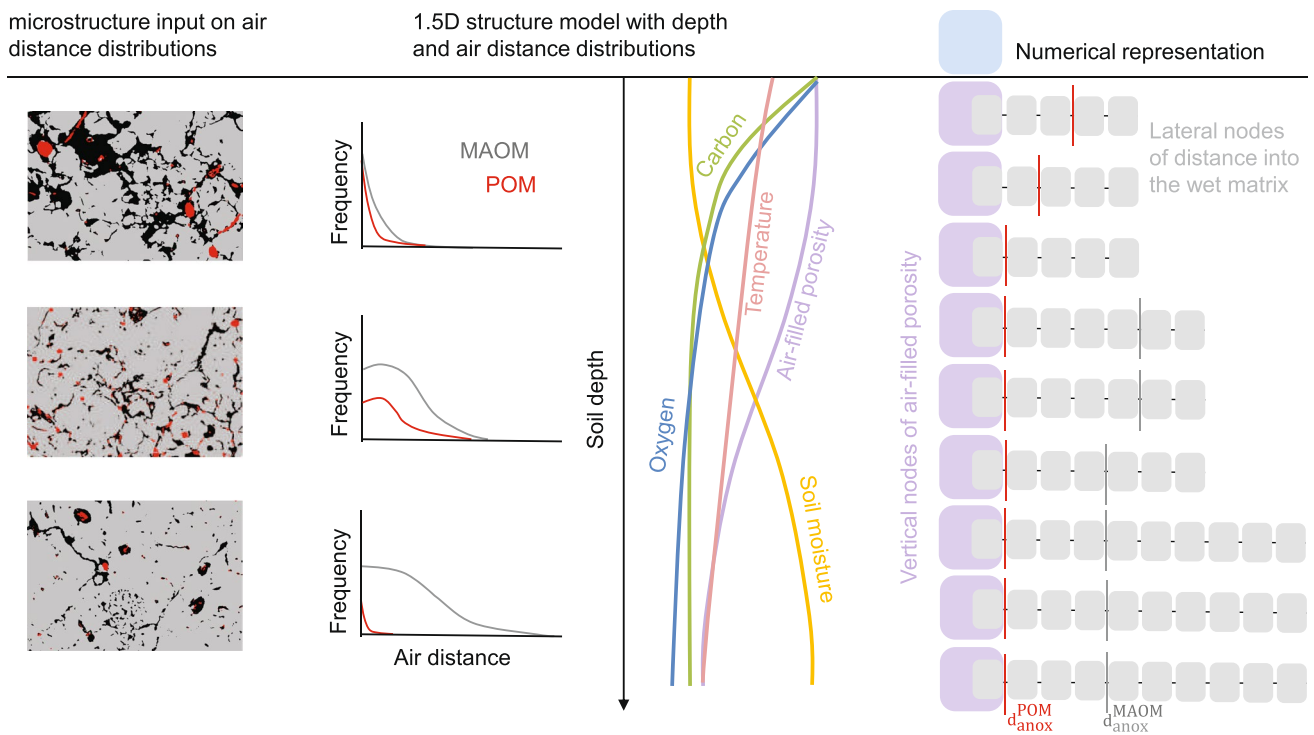
Fig. 7 Conceptual design of a 1.5-dimensional denitrification model at the soil profile-scale based on microstructure information (center). The model considers vertical gas transport in air and lateral transport of dissolved gases in the wet soil matrix (right). This lateral transport occurs in a distance domain with air-distance histograms of mineral-associated organic matter (MAOM) and particulate organic matter (POM) that are ideally derived from available microstructure information (left). The critical distances for the formation of anoxia in POM and MAOM, d_{anox}^{POM} and d_{anox}^{MAOM}, are either an outcome of the model or derived from empirical equations introduced in Sect. 3

matrix within a certain distance from the air-filled pores are at least statistically similar, and that meaningful average transport and reaction parameters exist for the distance class. Typically, we must rely on the assumption that organic carbon, nitrogen and the denitrification capacity of the microbial community is evenly distributed in space relative to the air-filled pores. However, if information on this distribution is available it can be incorporated into the model.

These local distance domain models are coupled to a traditional, vertical, one-dimensional model, where there is still a continuous gas phase to resolve gas exchange with the atmosphere. If there is no continuous gas phase in a layer or no gas phase at all, the orthogonal model is not necessary, as the distance to the next air-filled pore is now vertical and already resolved by the traditional one-dimensional model.

The new model allows the calculation of local anoxia and denitrification based on soil structural information and geochemical properties. The structural information is derived from undisturbed soil samples obtained by X-ray CT. A questionable idealization of the soil structure in the form of aggregates or cylindrical pores becomes obsolete. Moreover, the model places the concept of an anaerobic soil volume or anaerobic balloon on a spatially-explicit and clearer physico-chemical basis, while still being efficient enough

to be applied at the soil profile scale. The proposed concept is compatible with the soil profile scale models reviewed in Sect. 4, as the common depth-resolved state variables (Fig. 7) drive the orthogonal oxygen diffusion and consumption rates. Oxygen concentrations in the air-filled pore space act as a boundary condition for the lateral distance domain in each layer. A change in soil moisture and thus air-filled porosity affects both the downward movement of gaseous oxygen and the air distances through the wet matrix at each depth. Temperature affects both domains, whereas MAOM and POM are located in the distance domain either proportionally with air distances, according to available microscale information for a given soil layer (Fig. 7) or some other hypothetical distribution that could be tested in the framework of exploratory modeling. Information on dissolved, mineral-associated and particulate organic matter fractions is not routinely reported in denitrification studies, leaving profiles of total organic carbon as the only depth-resolved information of bioavailability of carbon substrates.

The mechanistic nature of this model could be fully harnessed by using substrate supply, e.g. calibrated with water-extractable organic carbon as the only input information on bioavailability, so that the local oxygen demand, the critical distance for the formation of anoxia (d_{anox}) and ultimately

the anaerobic soil volume fraction would arise as model outputs. Simplified versions are conceivable that use local oxygen demand as input information (if available) in order to estimate d_{anox} from the analytical or calibrated equations (Fig. 4) or from empirical equations with bulk soil properties as input parameters (Table 1). These also allow d_{anox} to be estimated separately for MAOM and POM.

The model requires distance distributions to air-filled pores as a function of water content. However, microstructure analyses of intact soil cores from all relevant soil depths, as shown in Fig. 6, are usually not available. An indirect approach outlined earlier would be to conceptualize the soil as a capillary bundle model and derive idealized distance distributions from water retention curves (Schurgers et al. 2006). Measuring water retention curves would again require intact soil cores from all soil depths considered, unless they are estimated from bulk soil properties with pedo-transfer functions (Carsel and Parrish 1988; Schaap et al. 2001). In the near future, another option would be to use air distance histograms from the Soil Structure Library (Weller et al. 2022). This is an open data repository where uploaded X-ray CT data of soil structure are analyzed according to a standardized pore space analysis protocol. Each uploaded dataset comes with meta-information such as soil type, land use, geographical coordinates, and soil depth, so that the library can be searched for specific settings and eventually used to build pedo-transfer functions.

Finally, we emphasize that such a model would only be suitable for upscaling microstructure information to the soil profile scale, as upscaling to the landscape scale presents a completely different set of problems (Groffman et al. 2009).

Conclusions

Denitrification activity on sub-cm to few-cm sized spatial scales and event-based temporal scales is mainly driven by anoxic microsites where all conditions for denitrification are met. This local concentration of denitrification in a fraction of the soil, called the anaerobic soil volume or anaerobic balloon, is a rather old concept that has been captured experimentally and implemented in models for more than thirty years. However, to date, the anaerobic soil volume has mostly been implemented as conceptual quantity which is calibrated to the observed denitrification, and few attempts have been made to physically capture it by independent observations or measurements. Accumulating experimental evidence indicates that the inherent properties of particulate organic matter and its distribution within the wet soil matrix, particularly its distances to air-filled pores, are the main drivers of denitrification activity, with little contribution from mineral-associated matter in the soil matrix. This was supported by meta-analyses of the controlling factors for i) microscopic air distance thresholds for anoxia formation

and ii) the apparent anaerobic soil volume fraction in oxic-anoxic incubations. Both meta-analyses indicated that bulk water and oxygen concentrations, which control the aeration of the soil matrix, do not predict denitrification activity well when this activity is concentrated in particulate organic matter, where the micro-environmental conditions partially decouple from the surrounding soil. Likewise, both meta-analyses confirmed each other in that soil organic carbon content was the single best predictor among basic soil properties for both target variables when pooled across all available data sets, but with low to moderate explained variability (R^2 of 0.27 and 0.41, respectively). In the future, more appropriate proxies for the abundance of labile carbon in soil should be added to standard reporting protocols of incubation studies. Candidates could be water-extractable organic carbon or particulate organic matter content derived from imaging or density fractionation. Furthermore, we identified considerable data gaps in both meta-analysis with a sample size of only $n = 61$ and $n = 76$, respectively. Building more robust statistical models requires much larger training datasets. This calls for (i) more standardized soil incubation studies that provide time series of $N_2O + N_2$ emission rates and complete reporting of essential soil properties according to the standard reporting framework of denitrification research (Almaraz et al. 2020) and (ii) more in-situ measurements of local oxygen gradients combined with a thorough characterization of soil properties to put the empirical equations introduced in this paper on a more solid basis.

Many common denitrification models relate the anaerobic soil volume fraction to the bulk oxygen concentration, which completely ignores the spatial concentration of denitrification activity in microbial hotspots. In addition, the exact implementation of this relationship varies among models, resulting in a wide variation of this anaerobic volume fraction for the same input, making it more of a calibration factor than a solid physical concept. A major obstacle to improving such models, which operate at relevant scales (meters – hectares), is that so far such microstructural information on air distances (μm – mm) of the wet soil matrix in general and of POM in particular is only available for a few experimental studies. A simple solution to account for microbial hotspots in denitrification models is to stochastically distribute oxygen availability. The more data-driven approach advocated in this review is to (i) conceptualize a soil profile as a vertical domain of fast gas transport in air-filled pores combined with lateral transport of dissolved gases in the wet soil matrix, (ii) establish new empirical relationships between the critical microscale distances for anoxia formation and several bulk properties common to all denitrification models, and (iii) to make an inventory of these distances for the most common combinations of soil textures and land uses. The establishment of such pedo-transfer functions has a long history in soil science, e.g. for soil hydraulic properties, and

huge databases for data assimilation based microstructure information are now emerging. Although the road ahead seems quite long at this stage, the gain in model accuracy from this big data driven approach could make a fundamental difference in predicting ephemeral denitrification events and changes in denitrification activity with land use change.

Data availability Spreadsheets containing the input data for the meta-analyses in Sect. 3.4 and 3.5 are available as Supplementary Data S1 and S2, respectively.

Declarations

Competing interests None declared.

References

Abbott MB, Bathurst JC, Cunge JA, O'Connell PE, Rasmussen J (1986) An introduction to the European Hydrological System — Systeme Hydrologique Europeen, "SHE", 2: Structure of a physically-based, distributed modelling system. J Hydrol 87:61–77. https://doi.org/10.1016/0022-1694(86)90115-0

Almaraz M, Wong MY, Yang WH (2020) Looking back to look ahead: a vision for soil denitrification research. Ecology 101:e02917. https://doi.org/10.1002/ecy.2917

Andersen AJ, Petersen SO (2009) Effects of C and N availability and soil-water potential interactions on N2O evolution and PLFA composition. Soil Biol Biochem 41:1726–1733. https://doi.org/10.1016/j.soilbio.2009.06.001

Angert A, Yakir D, Rodeghiero M, Preisler Y, Davidson EA, Weiner T (2015) Using O_2 to study the relationships between soil CO_2 efflux and soil respiration. Biogeosciences 12:2089–2099. https://doi.org/10.5194/bg-12-2089-2015

Arah JRM, Smith KA (1989) Steady-state denitrification in aggregated soils: a mathematical model. J Soil Sci 40:139–149

Arah JRM, Vinten AJA (1995) Simplified models of anoxia and denitrification in aggregated and simple-structured soils. Eur J Soil Sci 46:507–517. https://doi.org/10.1111/j.1365-2389.1995.tb01347.x

Bach EM, Williams RJ, Hargreaves SK, Yang F, Hofmockel KS (2018) Greatest soil microbial diversity found in micro-habitats. Soil Biol Biochem 118:217–226. https://doi.org/10.1016/j.soilbio.2017.12.018

Bakken LR, Bergaust L, Liu B, Frostegård Å (2012) Regulation of denitrification at the cellular level: a clue to the understanding of N2O emissions from soils. Philos Trans R Soc B 367:1226–1234. https://doi.org/10.1098/rstb.2011.0321

Balaine N, Clough TJ, Beare MH, Thomas SM, Meenken ED, Ross JG (2013) Changes in Relative Gas Diffusivity Explain Soil Nitrous Oxide Flux Dynamics. Soil Sci Soc Am J 77:1496–1505. https://doi.org/10.2136/sssaj2013.04.0141

Ball BC (2013) Soil structure and greenhouse gas emissions: a synthesis of 20 years of experimentation. Eur J Soil Sci 64:357–373. https://doi.org/10.1111/ejss.12013

Bateman EJ, Baggs EM (2005) Contributions of nitrification and denitrification to N2O emissions from soils at different water-filled pore space. Biol Fertil Soils 41:379–388. https://doi.org/10.1007/s00374-005-0858-3

Bergaust L, Bakken Lars R, Frostegård Å (2011) Denitrification regulatory phenotype, a new term for the characterization of denitrifying bacteria. Biochem Soc Trans 39:207–212. https://doi.org/10.1042/bst0390207

Bergstermann A, Cárdenas L, Bol R, Gilliam L, Goulding K, Meijide A, Scholefield D, Vallejo A, Well R (2011) Effect of antecedent soil moisture conditions on emissions and isotopologue distribution of N2O during denitrification. Soil Biol Biochem 43:240–250. https://doi.org/10.1016/j.soilbio.2010.10.003

Blagodatsky S, Smith P (2012) Soil physics meets soil biology: Towards better mechanistic prediction of greenhouse gas emissions from soil. Soil Biol Biochem 47:78–92. https://doi.org/10.1016/j.soilbio.2011.12.015

Blagodatsky S, Grote R, Kiese R, Werner C, Butterbach-Bahl K (2011) Modelling of microbial carbon and nitrogen turnover in soil with special emphasis on N-trace gases emission. Plant Soil 346:297. https://doi.org/10.1007/s11104-011-0821-z

Bocking CR, Blyth MG (2018) Oxygen uptake and denitrification in soil aggregates. Acta Mech 229:595–612. https://doi.org/10.1007/s00707-017-2042-x

Borer B, Tecon R, Or D (2018) Spatial organization of bacterial populations in response to oxygen and carbon counter-gradients in pore networks. Nature Comm 9:769. https://doi.org/10.1038/s41467-018-03187-y

Braker G, Conrad R (2011) Chapter 2 - Diversity, Structure, and Size of N2O-Producing Microbial Communities in Soils—What Matters for Their Functioning? Adv Appl Microbiol 75:33–70

Burgin AJ, Groffman PM, Lewis DN (2010) Factors Regulating Denitrification in a Riparian Wetland. Soil Sci Soc Am J 74:1826–1833. https://doi.org/10.2136/sssaj2009.0463

Burgin AJ, Groffman PM (2012) Soil O2 controls denitrification rates and N2O yield in a riparian wetland. J Geophys Res 117:G01010. https://doi.org/10.1029/2011JG001799

Butterbach-Bahl K, Baggs EM, Dannenmann M, Kiese R, Zech-meister-Boltenstern S (2013) Nitrous oxide emissions from soils: how well do we understand the processes and their controls? Philos Trans R Soc B 368:20130122. https://doi.org/10.1098/rstb.2013.0122

Cardenas LM, Bol R, Lewicka-Szczebak D, Gregory AS, Matthews GP, Whalley WR, Misselbrook TH, Scholefield D, Well R (2017) Effect of soil saturation on denitrification in a grassland soil. Biogeosciences 14:4691–4710. https://doi.org/10.5194/bg-14-4691-2017

Carsel RF, Parrish RS (1988) Developing joint probability distributions of soil water retention characteristics. Water Resour Res 24:755–769

Casey RE, Taylor MD, Klaine SJ (2004) Localization of denitrification activity in macropores of a riparian wetland. Soil Biol Biochem 36:563–569. https://doi.org/10.1016/j.soilbio.2003.11.003

Castellano MJ, Schmift JP, Kaye JP, Walker C, Graham CB, Lin H, Dell CJ (2010) Hydrological and biogeochemical controls on the timing and magnitude of nitrous oxide flux across an agricultural landscape. Glob Change Biol 16:2711–2720. https://doi.org/10.1111/j.1365-2486.2009.02116.x

Cavigelli MA, Robertson GP (2001) Role of denitrifier diversity in rates of nitrous oxide consumption in a terrestrial ecosystem. Soil Biol Biochem 33:297–310. https://doi.org/10.1016/S0038-0717(00)00141-3

Chamindu Deepagoda TKK, Jayarathne JRRN, Clough TJ, Thomas S, Elberling B (2019) Soil-Gas Diffusivity and Soil-Moisture effects on N2O Emissions from Intact Pasture Soils. Soil Sci Soc Am J 83:1032–1043. https://doi.org/10.2136/sssaj2018.10.0405

Čuhel J, Šimek M (2011) Proximal and distal control by pH of denitrification rate in a pasture soil. Agric Ecosyst Environ 141:230–233. https://doi.org/10.1016/j.agee.2011.02.016

Currie JA (1961) Gaseous diffusion in the aeration of aggregated soils. Soil Sci 92:40–45

Del Grosso SJ, Parton WJ, Mosier AR, Ojima DS, Kulmala AE, Phong-pan S (2000) General model for N2O and N2 gas emissions from soils due to dentrification. Glob Biogeochem Cycles 14:1045–1060. https://doi.org/10.1029/1999GB001225

Du Y, Guo S, Wang R, Song X, Ju X (2023) Soil pore structure mediates the effects of soil oxygen on the dynamics of greenhouse gases during wetting–drying phases. Sci Total Environ 895:165192. https://doi.org/10.1016/j.scitotenv.2023.165192

Ebrahimi A, Or D (2015) Hydration and diffusion processes shape microbial community organization and function in model soil aggregates. Water Resour Res 51:9804–9827

Ebrahimi A, Or D (2016) Microbial community dynamics in soil aggregates shape biogeochemical gas fluxes from soil profiles - upscaling an aggregate biophysical model. Glob Change Biol 22:3141–3156

Ebrahimi A, Or D (2018) On upscaling of soil microbial processes and biogeochemical fluxes from aggregates to landscapes. J Geophys Res Biogeosci 123:1526–1547. https://doi.org/10.1029/2017JG004347

Fierer N, Schimel JP (2003) A proposed mechanism for the pulse in carbon dioxide production commonly observed following the rapid rewetting of a dry soil. Soil Sci Soc Am J 67:798–805

Firestone M (1982) Biological denitrification. In: Stevenson FJ (ed) Nitrogen in agricultural soils. Am Soc Agron pp 289–326. https://doi.org/10.2134/agronmonogr22.c8

Friedl J, Scheer C, Rowlings DW, McIntosh HV, Strazzabosco A, Warner DI, Grace PR (2016) Denitrification losses from an intensively managed sub-tropical pasture – Impact of soil moisture on the partitioning of N2 and N2O emissions. Soil Biol Biochem 92:58–66. https://doi.org/10.1016/j.soilbio.2015.09.016

Friedl J, Cardenas LM, Clough TJ, Dannenmann M, Hu C, Scheer C (2020) Measuring denitrification and the N2O:(N2O+N2) emission ratio from terrestrial soils. Curr Opin Environ Sustain 47:61–71. https://doi.org/10.1016/j.cosust.2020.08.006

Friedl J, Scheer C, De Rosa D, Müller C, Grace PR, Rowlings DW (2021) Sources of nitrous oxide from intensively managed pasture soils: the hole in the pipe. Env Res Lett 16:065004. https://doi.org/10.1088/1748-9326/abfde7

Galloway JN, Dentener FJ, Capone DG, Boyer EW, Howarth RW, Seitzinger SP, Asner GP, Cleveland CC, Green PA, Holland EA, Karl DM, Michaels AF, Porter JH, Townsend AR, Vöosmarty CJ (2004) Nitrogen Cycles: Past, Present, and Future. Biogeochemistry 70:153–226. https://doi.org/10.1007/s10533-004-0370-0

Ghezzehei TA, Sulman B, Arnold CL, Bogie NA, Berhe AA (2019) On the role of soil water retention characteristic on aerobic microbial respiration. Biogeosciences 16:1187–1209. https://doi.org/10.5194/bg-16-1187-2019

Gillam KM, Zebarth BJ, Burton DL (2008) Nitrous oxide emissions from denitrification and the partitioning of gaseous losses as affected by nitrate and carbon addition and soil aeration. Can J Soil Sci 88:133–143. https://doi.org/10.4141/cjss06005

Groenendijk P, Renaud LV, Roelsma J (2005) Prediction of nitrogen and phosphorus leaching to groundwater and surface waters; process descriptions of the animo4.0 model. Alterra report, Wageningen p 983

Groffman PM, Altabet MA, Böhlke JK, Butterbach-Bahl K, David MB, Firestone MK, Giblin AE, Kana TM, Nielsen LP, Voytek MA (2006) Methods for measuring denitrification: diverse approaches to a difficult problem. Ecol Appl 16:2091–2122. https://doi.org/10.1890/1051-0761(2006)016[2091:MFMDDA]2.0.CO;2

Groffman PM, Butterbach-Bahl K, Fulweiler RW, Gold AJ, Morse JL, Stander EK, Tague C, Tonitto C, Vidon P (2009) Challenges to incorporating spatially and temporally explicit phenomena (hotspots and hot moments) in denitrification models. Biogeochemistry 93:49–77

Grosz B, Well R, Dechow R, Köster JR, Khalil MI, Merl S, Rode A, Ziehmer B, Matson A, He H (2021) Evaluation of denitrification and decomposition from three biogeochemical models using laboratory measurements of N2, N2O and CO2. Biogeosciences 18:5681–5697. https://doi.org/10.5194/bg-18-5681-2021

Guo X, Drury CF, Yang X, Daniel Reynolds W, Fan R (2014) The extent of soil drying and rewetting affects nitrous oxide emissions, denitrification, and nitrogen mineralization. Soil Sci Soc Am J 78:194–204. https://doi.org/10.2136/sssaj2013.06.0219

Heinen M (2006) Simplified denitrification models: Overview and properties. Geoderma 133:444–463. https://doi.org/10.1016/j.geoderma.2005.06.010

Højberg O, Revsbech NP, Tiedje JM (1994) Denitrification in soil aggregates analyzed with microsensors for nitrous oxide and oxygen. Soil Sci Soc Am J 58:1691–1698

Holtan-Hartwig L, Dörsch P, Bakken LR (2002) Low temperature control of soil denitrifying communities: kinetics of N2O production and reduction. Soil Biol Biochem 34:1797–1806. https://doi.org/10.1016/S0038-0717(02)00169-4

Iqbal A, Beaugrand J, Garnier P, Recous S (2013) Tissue density determines the water storage characteristics of crop residues. Plant Soil 367:285–299. https://doi.org/10.1007/s11104-012-1460-8

Iqbal J, Parkin TB, Helmers MJ, Zhou X, Castellano MJ (2015) Denitrification and Nitrous Oxide Emissions in Annual Croplands, Perennial Grass Buffers, and Restored Perennial Grasslands. Soil Sci Soc Am J 79:239–250. https://doi.org/10.2136/sssaj2014.05.0221

Jarecke KM, Loecke TD, Burgin AJ (2016) Coupled soil oxygen and greenhouse gas dynamics under variable hydrology. Soil Biol Biochem 95:164–172. https://doi.org/10.1016/j.soilbio.2015.12.018

Keiluweit M, Nico PS, Kleber M, Fendorf S (2016) Are oxygen limitations under recognized regulators of organic carbon turnover in

upland soils? Biogeochemistry 127:157–171. https://doi.org/10.1007/s10533-015-0180-6

Keiluweit M, Gee K, Denney A, Fendorf S (2018) Anoxic microsites in upland soils dominantly controlled by clay content. Soil Biol Biochem 118:42–50. https://doi.org/10.1016/j.soilbio.2017.12.002

Kim K, Guber A, Rivers M, Kravchenko A (2020) Contribution of decomposing plant roots to N2O emissions by water absorption. Geoderma 375:114506. https://doi.org/10.1016/j.geoderma.2020.114506

Kraus D, Weller S, Klatt S, Haas E, Wassmann R, Kiese R, Butterbach-Bahl K (2015) A new LandscapeDNDC biogeochemical module to predict CH4 and N2O emissions from lowland rice and upland cropping systems. Plant Soil 386:125–149. https://doi.org/10.1007/s11104-014-2255-x

Kravchenko AN, Toosi ER, Guber AK, Ostrom NE, Yu J, Azeem K, Rivers ML, Robertson GP (2017) Hotspots of soil N2O emission enhanced through water absorption by plant residue. Nature Geosci 10:496. https://doi.org/10.1038/ngeo2963

Kravchenko AN, Fry JE, Guber AK (2018a) Water absorption capacity of soil-incorporated plant leaves can affect N2O emissions and soil inorganic N concentrations. Soil Biol Biochem 121:113–119. https://doi.org/10.1016/j.soilbio.2018.03.013

Kravchenko AN, Guber AK, Quigley MY, Koestel J, Gandhi H, Ostrom NE (2018b) X-ray computed tomography to predict soil N2O production via bacterial denitrification and N2O emission in contrasting bioenergy cropping systems. GCB Bioenergy. https://doi.org/10.1111/gcbb.12552

Kuzyakov Y, Blagodatskaya E (2015) Microbial hotspots and hot moments in soil: Concept & review. Soil Biol Biochem 83:184–199

Lacroix EM, Mendillo J, Gomes A, Dekas A, Fendorf S (2022) Contributions of anoxic microsites to soil carbon protection across soil textures. Geoderma 425:116050. https://doi.org/10.1016/j.geoderma.2022.116050

Lacroix EM, Aeppli M, Boye K, Brodie E, Fendorf S, Keiluweit M, Naughton HR, Noël V, Sihi D (2023) Consider the Anoxic Microsite: Acknowledging and Appreciating Spatiotemporal Redox Heterogeneity in Soils and Sediments. ACS Earth Space Chem. https://doi.org/10.1021/acsearthspacechem.3c00032

Larsen M, Santner J, Oburger E, Wenzel WW, Glud RN (2015) O2 dynamics in the rhizosphere of young rice plants (Oryza sativa L.) as studied by planar optodes. Plant Soil 390:279–292. https://doi.org/10.1007/s11104-015-2382-z

Lashermes G, Recous S, Alavoine G, Janz B, Butterbach-Bahl K, Ernfors M, Laville P (2022) N2O emissions from decomposing crop residues are strongly linked to their initial soluble fraction and early C mineralization. Sci Tot Env 806:150883. https://doi.org/10.1016/j.scitotenv.2021.150883

Leuther F, Wolff M, Kaiser K, Schumann L, Merbach I, Mikutta R, Schlüter S (2022) Response of subsoil organic matter contents and physical properties to long-term, high-rate farmyard manure application. Eur J Soil Sci 73:e13233. https://doi.org/10.1111/ejss.13233

Li C, Frolking S, Frolking TA (1992) A model of nitrous oxide evolution from soil driven by rainfall events: 1. Model structure and sensitivity. J Geophys Res: Atm 97:9759–9776. https://doi.org/10.1029/92JD00509

Li C, Aber J, Stange F, Butterbach-Bahl K, Papen H (2000) A process-oriented model of N2O and NO emissions from forest soils: 1. Model Development J Geophys Res: Atm 105:4369–4384

Li C, Salas W, Zhang R, Krauter C, Rotz A, Mitloehner F (2012) Manure-DNDC: a biogeochemical process model for quantifying greenhouse gas and ammonia emissions from livestock manure systems. Nutr Cycl Agroecos 93:163–200. https://doi.org/10.1007/s10705-012-9507-z

Li Y, Clough TJ, Moinet GYK, Whitehead D (2021) Emissions of nitrous oxide, dinitrogen and carbon dioxide from three soils amended with carbon substrates under varying soil matric potentials. Eur J Soil Sci 72:2261–2275. https://doi.org/10.1111/ejss.13124

Li Z, Tang Z, Song Z, Chen W, Tian D, Tang S, Wang X, Wang J, Liu W, Wang Y, Li J, Jiang L, Luo Y, Niu S (2022) Variations and controlling factors of soil denitrification rate. Glob Change Biol 28:2133–2145. https://doi.org/10.1111/gcb.16066

Linn D, Doran J (1984) Effect of water-filled pore space on carbon dioxide and nitrous oxide production in tilled and nontilled soils. Soil Sci Soc Am J 48:1267–1272

Loecke TD, Robertson GP (2009) Soil resource heterogeneity in terms of litter aggregation promotes nitrous oxide fluxes and slows decomposition. Soil Biol Biochem 41:228–235. https://doi.org/10.1016/j.soilbio.2008.10.017

Lucas M, Schlüter S, Vogel H-J, Vetterlein D (2019) Roots compact the surrounding soil depending on the structures they encounter. Sci Rep 9:16236. https://doi.org/10.1038/s41598-019-52665-w

Lucas M, Santiago JP, Chen J, Guber A, Kravchenko A (2023b) The soil pore structure encountered by roots affects plant-derived carbon inputs and fate. New Phytol 240:515–528. https://doi.org/10.1111/nph.19159

Lucas M, Gil J, Robertson GP, Ostrom NE, Kravchenko A (2023a) Changes in soil pore structure generated by the root systems of maize, sorghum and switchgrass affect in situ N2O emissions and bacterial denitrification. Biol Fert Soils. https://doi.org/10.1007/s00374-023-01761-1

Lucas M, Rohe L, Apelt B, Stange CF, Vogel H-J, Well R, Schlüter S (2024) The distribution of particulate organic matter in the heterogeneous soil matrix - balancing between aerobic respiration and denitrification. bioRxiv: 2024.2003.2016.585355. https://doi.org/10.1101/2024.03.16.585355

Manzoni S, Schimel JP, Porporato A (2012) Responses of soil microbial communities to water stress: results from a meta-analysis. Ecology 93:930–938. https://doi.org/10.1890/11-0026.1

Meyer RL, Kjær T, Revsbech NP (2002) Nitrification and Denitrification near a Soil-Manure Interface Studied with a Nitrate-Nitrite Biosensor. Soil Sci Soc Am J 66:498–506. https://doi.org/10.2136/sssaj2002.4980

Micucci G, Sgouridis F, McNamara NP, Krause S, Lynch I, Roos F, Well R, Ullah S (2023) The 15N-Gas flux method for quantifying denitrification in soil: Current progress and future directions. Soil Biol Biochem 184:109108. https://doi.org/10.1016/j.soilbio.2023.109108

Millington R (1959) Gas diffusion in porous media. Science 130:100–102

Moyano FE, Manzoni S, Chenu C (2013) Responses of soil heterotrophic respiration to moisture availability: An exploration of processes and models. Soil Biol Biochem 59:72–85. https://doi.org/10.1016/j.soilbio.2013.01.002

Mutegi JK, Munkholm LJ, Petersen BM, Hansen EM, Petersen SO (2010) Nitrous oxide emissions and controls as influenced by tillage and crop residue management strategy. Soil Biol Biochem 42:1701–1711. https://doi.org/10.1016/j.soilbio.2010.06.004

Myrold DD, Tiedje JM (1985) Diffusional constraints on denitrification in soil. Soil Sci Soc Am J 49:651–657

Nielsen TH, Nielsen LP, Revsbech NP (1996) Nitrification and Coupled Nitrification-Denitrification Associated with a Soil-Manure Interface. Soil Sci Soc Am J 60:1829–1840. https://doi.org/10.2136/sssaj1996.03615995006000060031x

Norman J, Jansson P-E, Farahbakhshazad N, Butterbach-Bahl K, Li C, Klemedtsson L (2008) Simulation of NO and N2O emissions from a spruce forest during a freeze/thaw event using an N-flux submodel from the PnET-N-DNDC model integrated to CoupModel. Ecol Model 216:18–30. https://doi.org/10.1016/j.ecolmodel.2008.04.012

Ortega-Ramírez P, Pot V, Laville P, Schlüter S, Amor-Quiroz DA, Hadjar D, Mazurier A, Lacoste M, Caurel C, Pouteau V, Chenu C, Basile-Doelsch I, Henault C, Garnier P (2023) Pore distances of particulate organic matter predict N2O emissions from intact soil at moist conditions. Geoderma 429:116224. https://doi.org/10.1016/j.geoderma.2022.116224

Ostrom PH, DeCamp S, Gandhi H, Haslun J, Ostrom NE (2021) The influence of tillage and fertilizer on the flux and source of nitrous oxide with reference to atmospheric variation using laser spectroscopy. Biogeochemistry 152:143–159. https://doi.org/10.1007/s10533-020-00742-y

Owens J, Clough TJ, Laubach J, Hunt JE, Venterea RT (2017) Nitrous Oxide Fluxes and Soil Oxygen Dynamics of Soil Treated with Cow Urine. Soil Sci Soc Am J 81:289–298. https://doi.org/10.2136/sssaj2016.09.0277

Parkin TB (1987) Soil microsites as a source of denitrification variability. Soil Sci Soc Am J 51:1194–1199

Parkin TB, Tiedje JM (1984) Application of a soil core method to investigate the effect of oxygen concentration on denitrification. Soil Biol Biochem 16:331–334. https://doi.org/10.1016/0038-0717(84)90027-0

Petersen SO, Schjønning P, Thomsen IK, Christensen BT (2008) Nitrous oxide evolution from structurally intact soil as influenced by tillage and soil water content. Soil Biol Biochem 40:967–977. https://doi.org/10.1016/j.soilbio.2007.11.017

Petersen SO, Ambus P, Elsgaard L, Schjønning P, Olesen JE (2013) Long-term effects of cropping system on N2O emission potential. Soil Biol Biochem 57:706–712. https://doi.org/10.1016/j.soilbio.2012.08.032

Pett-Ridge J, Silver WL, Firestone MK (2006) Redox Fluctuations Frame Microbial Community Impacts on N-cycling Rates in a Humid Tropical Forest Soil. Biogeochemistry 81:95–110. https://doi.org/10.1007/s10533-006-9032-8

Philippot L, Hallin S, Schloter M (2007) Ecology of Denitrifying Prokaryotes in Agricultural Soil. Adv Agron 96:249–305. https://doi.org/10.1016/S0065-2113(07)96003-4

Philippot L, Andert J, Jones CM, Bru D, Hallin S (2011) Importance of denitrifiers lacking the genes encoding the nitrous oxide reductase for N2O emissions from soil. Glob Change Biol 17:1497–1504

Porre RJ, van Groenigen JW, De Deyn GB, de Goede RGM, Lubbers IM (2016) Exploring the relationship between soil mesofauna, soil structure and N2O emissions. Soil Biol Biochem 96:55–64. https://doi.org/10.1016/j.soilbio.2016.01.018

Rabot E, Lacoste M, Hénault C, Cousin I (2015) Using x-ray computed tomography to describe the dynamics of nitrous oxide emissions during soil drying. Vadose Zone J 14. https://doi.org/10.2136/vzj2014.12.0177

Reddy KR, Patrick WH, Broadbent FE (1984) Nitrogen transformations and loss in flooded soils and sediments. CRC Crit Rev Env Control 13:273–309. https://doi.org/10.1080/10643388409381709

Refsgaard JC, Christensen TH, Ammentorp HC (1991) A model for oxygen transport and consumption in the unsaturated zone. J Hydrol 129:349–369. https://doi.org/10.1016/0022-1694(91)90058-P

Rijtema PE, Kroes JG (1991) Some results of nitrogen simulations with the model ANIMO. Fert Res 27:189–198. https://doi.org/10.1007/BF01051127

Riley WJ, Matson PA (2000) NLOSS: a mechanistic model of denitrified N2O and N2 evolution from soil. Soil Sci 165:237–249

Robertson GP (2023) Denitrification and the challenge of scaling microsite knowledge to the globe. mLife 2:229–238. https://doi.org/10.1002/mlf2.12080

Robertson GP, Groffman PM (2007) 13 – Nitrogen transformations. In: Paul EA (ed) Soil Microbiology, Ecology and Biochemistry (Third Edition). Academic Press, San Diego, CA, p 552

Rohe L, Apelt B, Vogel HJ, Well R, Wu GM, Schlüter S (2021) Denitrification in soil as a function of oxygen availability at the microscale. Biogeosciences 18:1185–1201. https://doi.org/10.5194/bg-18-1185-2021

Rousset C, Clough TJ, Grace PR, Rowlings DW, Scheer C (2020) Soil type, bulk density and drainage effects on relative gas diffusivity and N2O emissions. Soil Res 58:726–736. https://doi.org/10.1071/SR20161

Rummel PS, Pfeiffer B, Pausch J, Well R, Schneider D, Dittert K (2020) Maize root and shoot litter quality controls short-term CO2 and N2O emissions and bacterial community structure of arable soil. Biogeosciences 17:1181–1198. https://doi.org/10.5194/bg-17-1181-2020

Ruser R, Flessa H, Russow R, Schmidt G, Buegger F, Munch JC (2006) Emission of N2O, N2 and CO2 from soil fertilized with nitrate: effect of compaction, soil moisture and rewetting. Soil Biol Biochem 38:263–274. https://doi.org/10.1016/j.soilbio.2005.05.005

Saggar S, Jha N, Deslippe J, Bolan NS, Luo J, Giltrap DL, Kim DG, Zaman M, Tillman RW (2013) Denitrification and N2O:N2 production in temperate grasslands: Processes, measurements, modelling and mitigating negative impacts. Sci Tot Env 465:173–195. https://doi.org/10.1016/j.scitotenv.2012.11.050

Schaap MG, Leij FJ, van Genuchten MT (2001) Rosetta: a computer program for estimating soil hydraulic parameters with hierarchical pedotransfer functions. J Hydrol 251:163–176

Schaufler G, Kitzler B, Schindlbacher A, Skiba U, Sutton MA, Zechmeister-Boltenstern S (2010) Greenhouse gas emissions from European soils under different land use: effects of soil moisture and temperature. Eur J Soil Sci 61:683–696. https://doi.org/10.1111/j.1365-2389.2010.01277.x

Schlatter DC, Reardon CL, Johnson-Maynard J, Brooks E, Kahl K, Norby J, Huggins D, Paulitz TC (2019) Mining the drilosphere: Bacterial communities and denitrifier abundance in a no-till wheat cropping system. Front Microbiol 10:1339. https://doi.org/10.3389/fmicb.2019.01339.

Schlesinger WH (2009) On the fate of anthropogenic nitrogen. Proc Nat Acad Sci usa 106:203–208. https://doi.org/10.1073/pnas.0810193105

Schlüter S, Zawallich J, Vogel HJ, Dörsch P (2019) Physical constraints for respiration in microbial hotspots in soil and their importance for denitrification. Biogeosciences 2019:1–31. https://doi.org/10.5194/bg-2019-2

Schlüter S, Albrecht L, Schwärzel K, Kreiselmeier J (2020) Long-term effects of conventional tillage and no-tillage on saturated and near-saturated hydraulic conductivity – Can their prediction be improved by pore metrics obtained with X-ray CT? Geoderma 361:114082. https://doi.org/10.1016/j.geoderma.2019.114082

Schlüter S, Leuther F, Albrecht L, Hoeschen C, Kilian R, Surey R, Mikutta R, Kaiser K, Mueller CW, Vogel H-J (2022) Microscale carbon distribution around pores and particulate organic matter varies with soil moisture regime. Nat Comm 13:2098. https://doi.org/10.1038/s41467-022-29605-w

Schurgers G, Dörsch P, Bakken L, Leffelaar P, Haugen LE (2006) Modelling soil anaerobiosis from water retention characteristics and soil respiration. Soil Biol Biochem 38:2637–2644. https://doi.org/10.1016/j.soilbio.2006.04.016

Senbayram M, Budai A, Bol R, Chadwick D, Marton L, Gündogan R, Wu D (2019) Soil NO3− level and O2 availability are key factors in controlling N2O reduction to N2 following long-term liming of an acidic sandy soil. Soil Biol Biochem 132:165–173. https://doi.org/10.1016/j.soilbio.2019.02.009

Senbayram M, Wei Z, Wu D, Shan J, Yan X, Well R (2022) Inhibitory effect of high nitrate on N2O reduction is offset by long moist spells in heavily N loaded arable soils. Biol Fert Soils 58:77–90. https://doi.org/10.1007/s00374-021-01612-x

Sexstone AJ, Revsbech NP, Parkin TB, Tiedje JM (1985) Direct measurement of oxygen profiles and denitrification rates in soil aggregates. Soil Sci Soc Am J 49:645–651

Shen W, Xue H, Gao N, Shiratori Y, Kamiya T, Fujiwara T, Isobe K, Senoo K (2020) Effects of copper on nitrous oxide (N2O) reduction

in denitrifiers and N2O emissions from agricultural soils. Biol Fert Soils 56:39–51. https://doi.org/10.1007/s00374-019-01399-y

Sierra J, Renault P (1995) Oxygen consumption by soil microorganisms as affected by oxygen and carbon dioxide levels. Appl Soil Ecol 2:175–184. https://doi.org/10.1016/0929-1393(95)00051-L

Sihi D, Davidson EA, Savage KE, Liang D (2020) Simultaneous numerical representation of soil microsite production and consumption of carbon dioxide, methane, and nitrous oxide using probability distribution functions. Glob Change Biol 26:200–218. https://doi.org/10.1111/gcb.14855

Silvennoinen H, Liikanen A, Torssonen J, Stange CF, Martikainen PJ (2008) Denitrification and N2O effluxes in the Bothnian Bay (northern Baltic Sea) river sediments as affected by temperature under different oxygen concentrations. Biogeochemistry 88:63–72. https://doi.org/10.1007/s10533-008-9194-7

Silver WL, Lugo AE, Keller M (1999) Soil oxygen availability and biogeochemistry along rainfall and topographic gradients in upland wet tropical forest soils. Biogeochemistry 44:301–328. https://doi.org/10.1007/BF00996995

Šimek M, Cooper JE (2002) The influence of soil pH on denitrification: progress towards the understanding of this interaction over the last 50 years. Eur J Soil Sci 53:345–354

Simojoki A, Jaakkola A (2000) Effect of nitrogen fertilization, cropping and irrigation on soil air composition and nitrous oxide emission in a loamy clay. Eur J Soil Sci 51:413–424. https://doi.org/10.1046/j.1365-2389.2000.00308.x

Skopp J, Jawson MD, Doran JW (1990) Steady-State Aerobic Microbial Activity as a Function of Soil Water Content. Soil Sci Soc Am J 54:1619–1625. https://doi.org/10.2136/sssaj1990.03615995005400060018x

Smith KA (1980) A model of the extent of anaerobic zones in aggregated soils, and its potential application to estimates of denitrification. J Soil Sci 31:263–277. https://doi.org/10.1111/j.1365-2389.1980.tb02080.x

Song X, Ju X, Topp CFE, Rees RM (2019) Oxygen Regulates Nitrous Oxide Production Directly in Agricultural Soils. Env Sci Tech 53:12539–12547. https://doi.org/10.1021/acs.est.9b03089

Stepniewski W (1980) Oxygen-diffusion and strength as related to soil compaction. I ODR Pol J Soil Sci 13:3–13

Stolk PC, Hendriks RFA, Jacobs CMJ, Moors EJ, Kabat P (2011) Modelling the effect of aggregates on N2O emission from denitrification in an agricultural peat soil. Biogeosciences 8:2649–2663. https://doi.org/10.5194/bg-8-2649-2011

Surey R, Schimpf CM, Sauheitl L, Mueller CW, Rummel PS, Dittert K, Kaiser K, Böttcher J, Mikutta R (2020) Potential denitrification stimulated by water-soluble organic carbon from plant residues during initial decomposition. Soil Biol Biochem 147:107841. https://doi.org/10.1016/j.soilbio.2020.107841

Surey R, Kaiser K, Schimpf CM, Mueller CW, Böttcher J, Mikutta R (2021) Contribution of particulate and mineral-associated organic matter to potential denitrification of agricultural soils. Front Env Sci 9. https://doi.org/10.3389/fenvs.2021.640534

Tian H, Xu R, Canadell JG, Thompson RL, Winiwarter W, Suntharalingam P, Davidson EA, Ciais P, Jackson RB, Janssens-Maenhout G, Prather MJ, Regnier P, Pan N, Pan S, Peters GP, Shi H, Tubiello FN, Zaehle S, Zhou F, Arneth A, Battaglia G, Berthet S, Bopp L, Bouwman AF, Buitenhuis ET, Chang J, Chipperfield MP, Dangal SRS, Dlugokencky E, Elkins JW, Eyre BD, Fu B, Hall B, Ito A, Joos F, Krummel PB, Landolfi A, Laruelle GG, Lauerwald R, Li W, Lienert S, Maavara T, MacLeod M, Millet DB, Olin S, Patra PK, Prinn RG, Raymond PA, Ruiz DJ, van der Werf GR, Vuichard N, Wang J, Weiss RF, Wells KC, Wilson C, Yang J, Yao Y (2020) A comprehensive quantification of global nitrous oxide sources and sinks. Nature 586:248–256. https://doi.org/10.1038/s41586-020-2780-0

Veraart AJ, de Klein JJM, Scheffer M (2011) Warming Can Boost Denitrification Disproportionately Due to Altered Oxygen Dynamics. PLoS ONE 6:e18508. https://doi.org/10.1371/journal.pone.0018508

Vogel H-J, Balseiro-Romero M, Kravchenko A, Otten W, Pot V, Schlüter S, Weller U, Baveye PC (2022) A holistic perspective on soil architecture is needed as a key to soil functions. Eur J Soil Sci 73:e13152. https://doi.org/10.1111/ejss.13152

Wagner-Riddle C, Congreves KA, Abalos D, Berg AA, Brown SE, Ambadan JT, Gao X, Tenuta M (2017) Globally important nitrous oxide emissions from croplands induced by freeze–thaw cycles. Nat Geosci 10:279–283. https://doi.org/10.1038/ngeo2907

Wang C, Amon B, Schulz K, Mehdi B (2021) Factors That Influence Nitrous Oxide Emissions from Agricultural Soils as Well as Their Representation in Simulation Models: A Review. Agronomy 11:770

Wei H, Song X, Liu Y, Wang R, Zheng X, Butterbach-Bahl K, Venterea RT, Wu D, Ju X (2023) In situ 15N–N2O site preference and O2 concentration dynamics disclose the complexity of N2O production processes in agricultural soil. Glob Change Biol 29:4910–4923. https://doi.org/10.1111/gcb.16753

Weier KL, Doran JW, Power JF, Walters DT (1993) Denitrification and the Dinitrogen/Nitrous Oxide Ratio as Affected by Soil Water, Available Carbon, and Nitrate. Soil Sci Soc Am J 57:66–72. https://doi.org/10.2136/sssaj1993.03615995005700010013x

Weller U, Albrecht L, Schlüter S, Vogel HJ (2022) An open Soil Structure Library based on X-ray CT data. SOIL 8:507–515. https://doi.org/10.5194/soil-8-507-2022

Werner C, Reiser K, Dannenmann M, Hutley LB, Jacobeit J, Butterbach-Bahl K (2014) N2O, NO, N2 and CO2 emissions from tropical savanna and grassland of northern Australia: an incubation experiment with intact soil cores. Biogeosciences 11:6047–6065. https://doi.org/10.5194/bg-11-6047-2014

Wösten JHM, Lilly A, Nemes A, Le Bas C (1999) Development and use of a database of hydraulic properties of European soils. Geoderma 90:169–185. https://doi.org/10.1016/S0016-7061(98)00132-3

Xu C, Wong VNL, Tuovinen A, Simojoki A (2023) Effects of liming on oxic and anoxic N2O and CO2 production in different horizons of boreal acid sulfate soil and non-acid soil under controlled conditions. Sci Tot Env 857:159505. https://doi.org/10.1016/j.scitotenv.2022.159505

Yang J, Feng L, Pi S, Cui D, Ma F, Zhao H-p, Li A (2020) A critical review of aerobic denitrification: Insights into the intracellular electron transfer. Sci Tot Env 731:139080. https://doi.org/10.1016/j.scitotenv.2020.139080

Zausig J, Stepniewski W, Horn R (1993) Oxygen Concentration and Redox Potential Gradients in Unsaturated Model Soil Aggregates. Soil Sci Soc Am J 57:908–916. https://doi.org/10.2136/sssaj1993.03615995005700040005x

Zhang J, Zhang W, Jansson PE, Petersen SO (2022) Modeling nitrous oxide emissions from agricultural soil incubation experiments using CoupModel. Biogeosciences 19:4811–4832. https://doi.org/10.5194/bg-19-4811-2022

Zhu X, Burger M, Doane TA, Horwath WR (2013) Ammonia oxidation pathways and nitrifier denitrification are significant sources of N2O and NO under low oxygen availability. Proc Nat Acad Sci usa 110:6328–6333. https://doi.org/10.1073/pnas.1219993110

Zhu K, Bruun S, Larsen M, Glud RN, Jensen LS (2015) Heterogeneity of O2 dynamics in soil amended with animal manure and implications for greenhouse gas emissions. Soil Biol Biochem 84:96–106. https://doi.org/10.1016/j.soilbio.2015.02.012

Zumft WG (1997) Cell biology and molecular basis of denitrification. Microbiol Mol Biol Rev 61:533–616. https://doi.org/10.1128/mmbr.61.4.533-616.1997